MEDICAL UNIVERSITY OF GRAZ

Thesis

MICRO CONDUCTION MEASUREMENTS OF CARDIAC FIBROSIS IN ISOLATED RAT HEARTS

Renata Grgic

12.09.2012

Doctoral thesis for obtaining the academic degree

Doctor of Medicine (Dr. med. Univ.)

Thesis

MICRO CONDUCTION MEASUREMENTS OF CARDIAC FIBROSIS IN ISOLATED RAT HEARTS

Doctoral thesis at the Medical University of Graz
for obtaining the academic degree

Doctor of Medicine (Dr. med. univ.)

Submitted by
Renata Grgic
Date of birth: 11.03.1983

Division of Transplant Surgery
Department of Surgery

Principal Supervisor:
Univ.-Prof. Dr. Andrä Wasler
Division of Cardiac Surgery
Department of Surgery

Second Supervisor:
Ass.-Dr. Michaela Schwarz
Division of Transplant Surgery
Section for Surgical Research
Department of Surgery

Graz, Date of Submission: September 12th , 2012

STATUTORY DECLARATION

I declare that I have authored this thesis independently, that I have not used other than the declared sources / resources, and that I have explicitly marked all material which has been quoted either literally or by content from the used sources.

Graz, 12.09.2012 .....

Signature

Acknowledgements

It would not have been possible to write this thesis without the help and support of the kind people around me, to only some of whom it is possible to give particular mention here.
Above all, I would like to thank my family for their personal support and great patience at all times. My friends and colleagues have given me their unequivocal support throughout, as always, for which my mere expression of thanks likewise does not suffice.
This thesis would not have been possible without the help, support and patience of my principal supervisor, Univ.-Prof. Dr. Andrä Wasler. The good advice, support and friendship of my second supervisor, Dr Michaela Schwarz, has been invaluable on both an academic and a personal level, for which I am extremely grateful.
Finally, this thesis would not have been possible without the help of several individuals who in one way or another contributed and extended their valuable assistance in the preparation and completion of this study:
ao.Univ.-Prof. Dipl.-Ing. Dr.techn. Ernst Hofer; Institute of Biophysics, Medical University of Graz
Dipl. Ing. Robert Arnold; Institute of Biophysics, Medical University of Graz
Dipl.-Ing. Thomas Wiener; Institute of Biophysics, Medical University of Graz
Univ.Doz. Dr. Meinitzer Andreas; Clinical Institute of Medical and Chemical Laboratory Diagnostics, Medical University of Graz
Dr.Martin Aßlaber; Clinical Institute of Pathology

This thesis is dedicated to my family, for their unwavering support and encouragement over the years.

Zusammenfassung

Ein Hauptrisikofaktor für die Ausprägung kardiovaskulärer Erkrankungen, die weltweit die Todesursache Nummer eins darstellen, ist die Entstehung von Fibrose.
Vorallem Herzrhythmusstörungen stehen in enger Korrelation mit der Art und dem Ausmaß der interstitiellen Fibrose.
Bis heute beeinflusst die Tatsache, dass Mikrofibrose mit den konventionellen diagnostischen Methoden derzeit nicht nachweisbar ist, den Erfolg bei der Katheterablation.

Die Hauptfragestellung der vorliegenden Studie beschäftigte sich damit, ob Mikrofibrose durch spezielle Cardiac Near Field Messungen elektrophysiologisch detektiert und in weiterer Folge auch quantifiziert werden könnte. Dazu wurde ein speziell entwickelter Sensor an isolierten Langendorff perfundierten Rattenherzen ausgetestet, nachdem Fibrose in 6 Versuchstieren durch chronische Cyclosporingabe induziert worden war. (die unbehandelte Kontrollgruppe bestand aus 4 Versuchstieren)
Zusätzlich zu den biophysikalischen Parametern wurden auch die physiologischen Parameter der isoliert schlangen Herzen evaluiert und aufgezeichnet.
In 50% der mit Cyclosporin behandelten Tiere wurde histopathologisch Fibrose nachgewiesen und dies auch elektrophysikalisch detektiert.Folgende Parameter zeigten signifikante Unterschiede: Eine Verminderung von $\Phi_e(t)$($p= 0,029$) und $d\Phi_e(t)/dt$ ($p= 0,002$), sowie eine Erhöhung des Fraktionierungsindexes innerhalb der Cyclosporingruppe.
Weitere Studien werden einerseits benötigt, um die vorliegenden Resultate zu untermauern und andererseits, um diese auch besser interpretieren zu können. Wir hoffen, dass durch die Weiterentwicklung dieser Methodik, die Diagnostik von Mikrofibrose möglich sein wird, um die aktuellen Therapiemöglichkeiten zu verbessern.

Abstract

Cardiac diseases are the leading cause of mortality throughout the world. Fibrosis is an important structural substrate leading to various cardiovascular pathologies. The quantity and the quality of fibrosis strongly correlate with the appearance of rhythm disorders. Especially micro fibrosis could not be efficiently detected up to now, thus limiting the accuracy of catheter ablation.
The present study aimed to detect micro fibrosis via cardiac near field measurement –for the first time in isolated perfused Langendorff rat hearts. Micro-conduction mapping methods as well as physiological measurements were performed on native (n=4) and on cyclosporine treated (n=6) rat hearts.
The main objective was to show if a possible correlation between the morphology of electrograms and the amount of underlying fibrosis induced by cyclosporine treatment, could be estimated.
In 50% of the cyclosporine treated rats, areas of minimal fibrosis were histopathologically confirmed. As expected this did not significantly affect the physiological cardiac performance. Nevertheless these minor structural changes could be detected through micro –conduction mapping using a new developed sensor. Significant differences were found. Following biophysical parameters: $\Phi_e(t)$($p= 0{,}029$), $d\Phi_e(t)/dt$ ($p= 0{,}002$) were decreased, while the fractionation index was higher in the cyclosporine treated group.
Although these findings need to be confirmed in future studies, they strongly imply the possibility to detect micro fibrosis and thereby offer a reasonable potential to be transferred into a clinical application.

The List of Abbreviations

AF	atrial fibrillation
bpm	beats per minute
BW	body weight
°C	degrees Celsius
CaCl2 2H2O	calcium chloride dihydrate
CF	coronary flow
CFAE	complex fractionated electrograms
CNF	cardiac near field
CsA	cyclosporine
CT	computer tomography
CVD	cardiovascular disease
D+	glucose anhydrous
dB	decibel
$d\Phi_e(t)/dt$	max negative peak voltage (from zero to the negative maximum) in the first temporal deviation of the extracellular potential Φ(V/s)
ECG	electrocardiogram
eNOS	endothelial nitric oxide synthase
Emag	maximum derived magnitude of cardiac near field strength (V/m)
ERP	effective refractory period
FI	fractionation index: number of deflections in dΦ/dt
GFR	glomerular filtration rate
GDP	gross domestic product
HE	hematoxylin eosin
hERG	human ether- a-go-go related gene
HR	heart rate
iNOS	inducible nitric oxide synthase

IS	immunosuppression
K^+	potassium
KCl	potassium chloride
kHz	kiloherz
KH2PO4	potassium dihydrogen phosphate
KRS	Krebs Ringer solution
LAT	local activation time
LCV	local conduction velocity
LGE-MRI	late gadolinium enhanced magnetic resonance imaging
MgSO4 7H2O	magnesium sulphate 7 hydrate
MPTP	mitochondrial permability transition pore
MRI	magnetic resonance imaging
NaCl	sodium chloride
NaHCO3	sodium hydrogen carbonate
$NO^{\cdot}$	nitric oxid
PDGF	platelet derived growth factor
RAAS	renin angiotensin aldosterone system
RONS	reactive oxygen and nitrogen species
rpm	rounds per minute
sHSPs	small heat shock proteins
SNR	signal to noise ratio
WHO	world health organisation
$\Phi_e(t)$	peak-to-peak voltage of the extracellular potential Φ(mV)

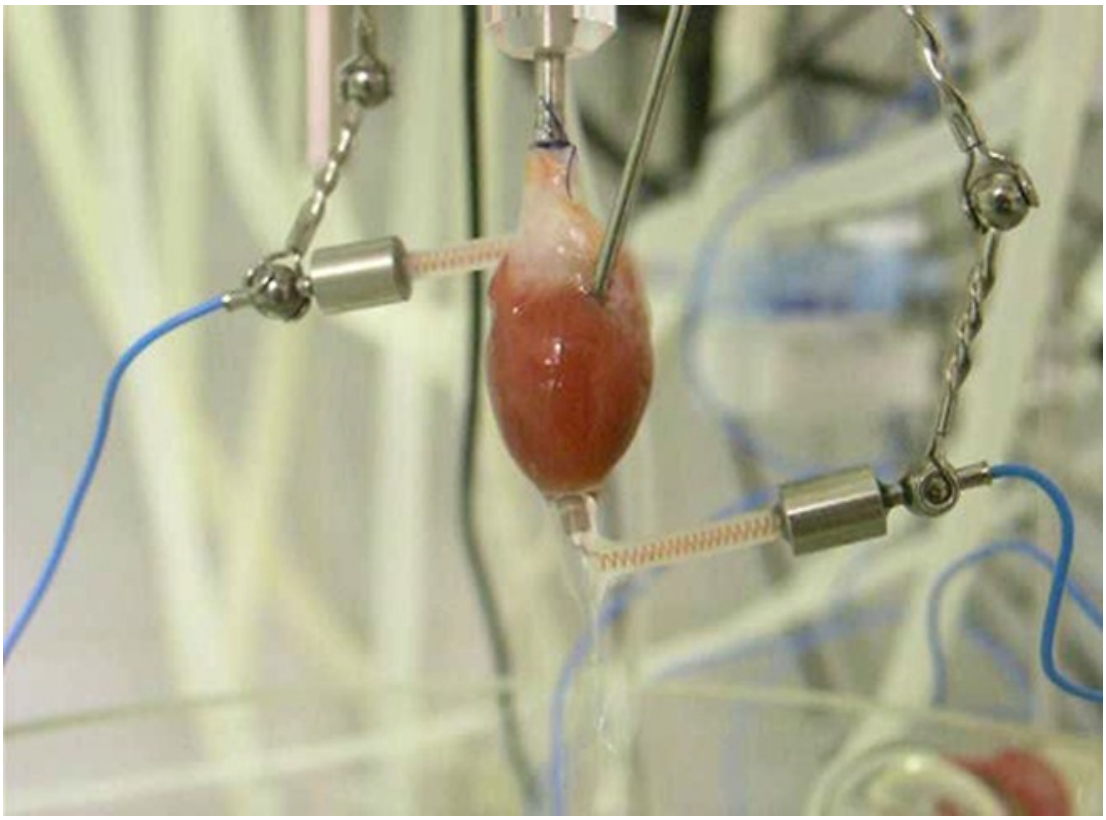

Isolated Heart Preparation, July 2010, Langendorff Apparatus, Section for Surgical Research

Summary

1) INTRODUCTION

1. 1 Myocardial Infarction and Fibrosis

1.1.1 Incidence of Cardiovascular Diseases

According to the latest European cardiovascular disease statistic from 2008 cardiovascular disaeses are the cause of death for 4.3 Million inhibitants yearly across Europe. CVD is the leading cause of death in the EU as well. Inside the EU 2 million deaths due to CVD are recorded annually and follow up costs for CVD patients of 192 billion per year have been named (1). Of those costs 57% are attributed to health care services (2).The situation in Austria is quite similar. A recent WHO statistics reported 399,4 deaths per 100.000 inhibitants per year (3). If all costs caused by CVD patients would be attributed to the gross domestic product – costs in Austria would be 11% of the GDP. This means that Austria would globally have the 8th position referring to the costs . (4) According to the latest death statistics it takes rank 7 for its present CVD mortality (5). In 2010 CVD was even found to be the most frequent cause of death in Austria (6).

According to the ICD 10 CVD can be divided into different subgroups (7), of which the ischemic heart disease, according to WHO statistics (8), takes the first place in Austria and equally in other countries.

1.1.2 Heart Fibrosis

Pathophysiology

Cardiovascular disease is a global problem – underlined by the fact that one third of the yearly mortality can be attributed to it. Most common cardiovascular death causes are coronary artery disease and stroke. Among coronary diseases myocardial infarction is the major cause of death and disability worldwide.
Myocardial infarction causes myocardial ischemia which leads to myocardial necrosis. The regional myocardial ischemia and hypo perfusion cause a cascade of events that finally ends in myocardial dysfunction and myocardial cell death and fibrosis (9) .

Fibrosis can mostly be found in ischemic scar tissue, but it can also occur in an absence of ischemia caused by a variety of other heart diseases. Every time fibrosis develops it does via an increase in collagen I and III synthesis by myofibroblasts. (10)
The collagen amount is not static, but is continuously synthesised and degraded.
In cardiac diseases, the equilibrium between collagen synthesis and breakdown is disturbed, resulting in collagen deposition i.e. collagen turnover (11). Fibrosis develops when circulating mediators, which are locally synthetized profibrotic factors, act on cardiac cells and increase collagen production without activating the increase of collagen degradation.
An increase in collagen deposition has been observed in the majority of CVD. This increase of fibrosis occurs as accumulation of collagen as replacement for necrosis or apoptosis of myocytes in order to protect the integrity of the heart and to compensate the ventricular function. Collagen deposition as a result of wound healing response to injury or cell death is observed in myocardial infarction, inflammation and Chagas disease.

An increase in the hearts´ collagen compound is not only observed in the diseases mentioned above, but also in aging hearts. Atrial fibrosis is a common endpoint in a variety of settings of the senescence heart. With aging, an intermolecular crosslinking of collagen increases, leading to myocardial stiffness and partly separation of myocardial bundles.
Furthermore, as a result of increased growth factor expression hypertrophic reactive fibrosis occurs. The amount of fibrosis differs among the various diseases.
It has also been discussed that the mentioned collagen increase might be caused by some channelopathies: for example a reduction of sodium channel expression has been shown in human Brugada syndrome; furthermore mutation of connexine channels has been proven in experimental studies of rats and mice. In addition several studies showed a downregulation of connexins in fibrosis replacement zones and chronically ischemic myocardium. (12)
Cardiac pathology is associated with two main mechanisms: enhanced structural remodelling and simultaneous decreased conexine expression.
(13) (14)
Although it has been proven that fibrosis causes a variety of CVD, the precise mechanism and pathway in fibrosis developing is yet unknown. It is estimated, that the atrium is more involved in occurrence of fibrosis than the ventricle. Three pathways seem to be involved in development of fibrosis including the hormonal axis -with renin angiotensin aldosterone (RAAS), growth factor overexpression and oxidative stress.
(12) (15)
Several studies showed that renin –angiotensin –aldosterone overexpression leads to the development of fibrosis, and furthermore that angiotensin converting enzyme inhibitors are able to regress myocardial fibrosis. The RAAS is involved in myocardial fibrosis development in hypertensive heart disease, chronic heart failure, myocardial infarction and cardiomyopathies. There is evidence that increased aldosterone or angiotensin cause AF.
Patients with idiopathic dilated cardiomyopathy benefit from a mineralocorticoid receptor antagonist treatment, which reduces left ventricular stiffness. (14)

Furthermore growth factors like the transforming growth factor ß1, who is the primary downstream mediator of angiotensin II, have as well an influence on fibrosis development. Transforming factor ß1 enhances the production of collagen and its overexpression causes atrial fibrosis. The platelet derived growth factor (PDGF) is discussed to play a role in fibrosis formation after inflammation. (12)
Adverse effects of some medications contribute to the development of CVD mostly through an increase of cardiac fibrosis. (16)
Nevertheless these drugs are essential for the treatment of specific diseases and the side effects are dependent on dosage and duration of their application.
Substances, which hold a potential to suppress NO synthesis are mostly considered to activate cardiac fibrosis progression.
In the field of organ transplantation the administration of immunosuppressants, especially cyclosporine (CsA) has a big impact on fibrotic genesis. (17)

Until now we do not have a full understanding of the precise mechanism leading to cardiac fibrosis and its progression. For more than 100 years animal models have been providing an important insight. The main progression happened within the past decades, showing that heterogeneity in tissue architecture disturbs ventricular function and may lead to development of arrhythmia. (18)

Types of Fibrosis

There are several ways to classify and divide fibrosis:
Reactive fibrosis occurs in absence of cardiomyocytes necrosis and cell loss, due to increased mechanical load, whereas replacement fibrosis or scarring is related to tissue and cell death. (11) (18)
Furthermore, histo-morphologically fibrosis can be described as interstitial, compact, patchy or diffuse:
-interstitial fibrosis comprises the extracellular matrix, develops mostly as reactive fibrosis and is often homogenously distributed throughout the tissue
-compact fibrosis comprises the fibrotic area of dense collagen which is completely deprived of intact myocardium. This type has the highest arrhythmogenic potential of all.
-patchy fibrosis is characterized by intermingle of collagen and myocardial bundles, forming compact strings of fibrosis.
-diffuse fibrosis consists of short stretches of fibrosis which are distributed throughout the tissue (14) (19)

According to the Utah classification fibrosis can be divided in 4 categories depending on its percentage relative to the left atrium wall volume, quantified by MRI :
Utah Stage 1 <5% →minimal
Utah Stage 2 >5–20% →mild
Utah Stage 3 >20–35% →moderate
Utah Stage 4 >35% →extensive
(20)

The Clinical Impact of Fibrosis

The importance of fibrosis in aetiology of cardiovascular diseases underlies the fact that fibroblasts actually outnumber the amount of cardiomyocytes within the heart, producing extracellular matrix. Excessive deposition of fibrotic tissue results in reduction of ventricular compliance and increase ventricular stiffness, which is correlated to a decreased volume fraction. A two to threefold increase in the collagen compound results in improper myocyte relaxation, leading to impairment of ventricular filling and filling pressure.
A minimisation of the stroke volume and an increased myocardial oxygen demand results in systolic and diastolic dysfunction, furthermore collagen deposition plays a major role in the formation of arrhythmias. (21)
Electrical, contractile and structural remodelling mainly contribute to the development and persistence of atrial fibrillation, in laboratory animals and humans.
Persisting atrial fibrillation promotes progressive atrial dilatation and functional impairment such as reduced contractility and atrial compliance. (12) (22)

Heart Fibrosis & Arrhythmia

According to the WHO, cardiac arrhythmias can be classified as another subtype of CVD. (23) Among them, atrial fibrillation (AF) is the most common dysrhythmia. It can be assumed, that the prevalence of AF, due to the presently aging population, improved cardiovascular therapies and longer survival rates, will increase in the upcoming years. According to the Framingham study there are trends indicating that in the year 2050 there may be about 16 million AF patients in the US. A similar increase can be estimated for other western countries. As a risk factor structural and functional alterations were indicated, as detected in patients with coronary artery disease and after cardiac surgery. (24) (25) (26) (27) (28)

The most common settings for atrial fibrillation are hypertension and ischemic heart disease; furthermore congestive heart failure might induce AF. Structural heart diseases are accompanied with the occurrence of changes in the refractory period and electrical propagation that increases the risk for arrhythmias.

Various studies have shown that fibrosis plays an important role in cardiac arrhythmias, in both, the ventricular and atrial level. (13)

A correlation of the extent of fibrosis and the persistence of the arrhythmias has been found in biopsies and autopsies of patients. (12)

Throughout all studies, it was recognised that increased tissue mass, short refractory period, slow conduction, regional conduction barriers, and electrical heterogeneity supported by vagal activation promoted arrhythmias.

In aging population a significant loss in myocardial fibres and an increase in fatty metamorphosis and connective tissue in the sinus node and atrium were detected. Even the arrhythmogenicity of pulmonary veins is partially given through the significantly fibrotic tissue in this area. (15) (29) (30)

Among the different types of fibrosis the arrhythmogenicity varies.

In compact fibrosis, re-entry mechanisms occur as circuit movement around the fibrotic area thus causing arrhythmias - dependent on the size of fibrosis, the conduction velocity, the refractory period and unidirectional block occurrence inside the myocardium. In case of a patchy fibrosis a conduction delay and a zig zag conduction between different bundles occurs around the fibrotic area, which is highly vulnerable to the development of arrhythmias.

Diffuse fibrosis affects the conduction disturbances in a far lesser extent than patchy fibrosis even if the amount is the same.

The arrhythmogenic substrate is defined as intermingle of fibrosis and myocardium, i.e. intermingle of electrically passive and active tissue results in asynchronous conduction and generates fractionation in electrograms. (22)

Animal models have provided a close insight into electrical mechanisms leading to atrial fibrillation:

Several theories have been established starting with the hyperectopical followed by the complementary single rotor theory; the theory of multiple circuit re-entries, of single rapid circuit and the theory of multiple wavelet circles which implicates that wavelength has to be less than the available circuit for re-entry to happen.

Finally the theories of focal sources, leading circles and spiral wave were established.

Which mechanism is specific for atrial fibrilation is yet unknown; although different studies indicate different mechanisms, there is mainly evidence for the re-entry and single foci theory.

In the most common theory of re-entrant circuit, a re-entry tachycardia persists due to a preformed re-entry pathway within the myocardium. This pathway is formed by conducting tissue around a barrier that slows or blocks conduction in one direction, i.e. an area of myocardium with a long refractory period intermingled with normal myocardium.

This barrier can be functional, consisting of conductive myocardium tissue that can develop a conduction block under some circumstances. Such tissue has a preferential conduction in one direction due to fibre orientation and mostly a transverse conduction is blocked with occurrence of rapid rates. The barrier can also be anatomic, i.e. pre-existing structures (like crista terminalis), scars from surgical incisions or inflammatory and degenerative conditions affecting the myocardium. Increased interstitial fibrosis separates myocardial bundles and impairs transverse conduction, while the longitudinal conduction is not affected. Therefore the conduction propagation becomes asynchronous.

The activation has to follow the tortuous route between collagen fibres which are to be considered as electrical barriers. Therefore the duration of the depolarisation is increased. This results in a reduced conduction velocity across transversal fibre direction. In case of a longitudinal direction, the conduction velocity stays near to normal. If the conduction is blocked one way, conduction propagation by an alternative pathway develops. This means that the conduction blocks distal from the harmed myocard and re-entries occur proximal to it– causing arrhythmias. (14) (15) (30) (31)

The effective refractory period (ERP) decrease is related to a collagen/fibrosis increase inside the myocardium. The electrical load of a fibroblast that is passed from this fibroblast to a cardiomyocyte increases an ERP whereas collagenous tissue matrix and its electric charge is lower than the myocards which might reduce the ERP.
Tissue discontinuities caused by fibrosis can also lead to initiation of spiral waves.
Fibrosis does not only play an important role in developing re-entry arrhythmias, but also in the occurrence of arrhythmias based on abnormal impulse generation through uncoupling such as automaticity and triggered activity.
Myocytes with the ability of spontaneous impulse generation may be silenced when tightly coupled to surrounding myocardium by having membrane potentials that are more negative. This can be changed by uncoupling the pacemaker cells from surrounding non pacemaker cells, which can be achieved by decreasing connexin expression or increasing collagen deposition, separating the cells electrically. The loss of side connections increases the transverse resistance and alters the properties of transverse conduction. Decrease in cell to cell coupling reduces conduction velocity, and promotes arrhythmias. (21)

Fibrosis is an attractive therapeutical target for the reduction of arrhythmogenicity.
Better insight in fibrosis development and detection may lead to an improvement of predicting the risk for arrhythmias and their treatment. It is a fact that available therapies are still suboptimal nowadays.
(14) (22)

1.1.3 Detection of Fibrosis → State of the Art

Invasive and non-invasive measurement of myocardial structure is limited through the lack of suitable methods. Different methods including imaging and biomarker analysis exist and are used to determine the presence, amount, and turnover of myocardial fibrosis.
However, the quantitative analysis of these techniques is not yet standardised. (22)
Nevertheless accurate detection of cardiac fibrosis as well as its progression is of crucial importance for an appropriate prognosis and therapy, and thereby of clinical importance. (9)
Numerous invasive and non-invasive methods for fibrosis detection exist and will be described below.

The cardiac biopsy as an invasive method is used to make accurate histo-morphological investigation of the structural changes, though this method is accompanied with the risk of perforation. Another disadvantage is that the biopsy only provides a highly localised insight into cardiac architecture. In cases where the samples are not collagen specific, immune histological or biochemical analysis can be performed.
A number of other methods are still in development and further research is needed. Antibody analysis for example is to date considered to be too expensive. Auto fluorescence methods may interfere with the quantitative analysis of fibrosis. A new bacterial protein, CNA35, is currently tested in its collagen binding affinities. Other biomolecules, such as the hydroxyprolin assay, are under investigation to be used to delineate collagen level. Nevertheless further research is needed to make these methods more accessible and accurate.
The determination of circulating biomarkers, such as breakdown protein products of collagen, could also be used to estimate the amount of collagen. Their use is simple, cheap and non-invasive but limited because the biomarkers are not specific to intra-cardiac collagen. Therefore valid statements about the amount of cardiac fibrosis are not significant. (19)

Late gadolinium enhanced magnetic resonance imaging (LGE-MRI) as a leading non-invasive method of fibrosis detection, has a completely different approach to fibrosis detection. This method is based on differences in washout kinetics of scar and viable tissue. Namely the areas of late enhancement of gadolinium correlate well with areas of fibrosis and thereby enable the differentiation between transmural and subendocardial scars on one hand and normal tissue on the other hand. Disadvantage of this method is that only larger areas of scars can be detected, while for small patches or interstitial fibrosis imaging is not possible, due to the fact that the fibrotic process is often diffuse and that there is a lack of a non-fibrotic myocardium as reference tissue. Further limitations of MRI are metallic implants and the fact that for high frequency arrhythmias (tachycardia) the image quality is limited due to scanning time. The same limitations are present during CT scans.

Echocardiography can be used to estimate the amount of fibrosis, through video-densitometry and texture analysis.

Myocardial fibrosis is associated with heterogeneity of conduction and therefore it affects the electrocardiogram (ECG) showing fractionation in areas where collagen and myocardium intermingles. The fractionation is significant especially in cases where electrical impulse propagation is perpendicular to fibre direction resulting in multiple deflections. However, in cases where the propagation is parallel to the fibrotic inlays, activation of the surrounding viable myocardium will be synchronous and only non-fractionated electrograms will be recorded. Fractionated electrograms are used to identify targets for catheter ablation. (10) (11) (13) (14)

Catheter Ablation → Importance of Accurate Fibrosis Detection and Mapping

Therapeutic options in case of arrhythmias are rhythm and frequency control. Antiarrhythmic drug therapy has its limitations.

In cases where drug therapy does not lead to improvement or is due to adverse effects not tolerated by patients, the catheter ablation is considered as a valuable option. Considering comorbidities and age of the patients the therapeutic approach has to be chosen individually.

Mapping and ablation methods are based on identifying the underlying primary cardiac pathology leading to fibrillation. Mainly, arrhythmias are caused by localized scar tissue and fibrosis, caused by ischemic or non-ischemic factors. (31) (32)

In the 1980's a surgical ablation therapy was developed for the treatment of ventricular tachycardia. With further insight of re-entry, slow conduction, and by identifying potential targets for interventions, catheter ablation was developed. This technique was improved by considering anatomical structures. New approaches with use of electro-anatomical mapping are used nowadays. (33)

New mapping procedures allow the ablation even if unstable tachycardia is present and should be considered as a therapeutic option before implanting a cardioverter or defibrillator. In experienced centres where the catheter ablation can be considered as a routine intervention, it shows to be a secure and effective therapy with good results being effective in 80% of the cases and having a low complication rate.

Disadvantages of this therapy are that often more than one ablation attempt is needed, and that the procedure is often applied by inexperienced medical staff.

New approaches include cryoablation or laser ablation and mapping methods including optical and electrical mapping. (13) (30)

Fibrosis Mapping

Intermingle of conducting myocardial and fibrotic tissue which is likely to induce arrhythmia, complicates ablation attempts. For successful termination of complex heart rhythm disorders by catheter ablation adequate mapping methods are needed. (31)
Different approaches to this issue were made over the years.
A century ago the first attempts for electric mapping of the heart were undertaken. It all started with Einthoven's ECG recording. Significant improvement was achieved around 50 years ago using isolated hearts in an experimental Langendorff setting.

Recent advantages are attributable to the progress in the multisite signal recording process. Different kinds of electrical mapping are described according to impulse detection: activation mapping, pace mapping, entertainment or substrate mapping. According to the impulse onset, endocardial and epicardial approaches are differentiated.
Endocardial methods include open heart models, plunge needle, endocardial basket and endocardial catheter mapping.
Epicardial mapping methods and endovascular catheter mapping such as Carto and EnSite NavX most commonly find their clinical application.
All electrical mapping methods have some limitations including low signal to noise ratio, inability to detect repolarisation of excitation and inability to record signals from several measurement sites simultaneously.
Due to these limitations optical mapping methods were developed, using voltage sensitive dyes which provide optical signal through luminescence that correlate with action potential and allow a precise evaluation of excitation propagation. The limitations of this method are underlying artefact problems and potential dye toxicity. (34)

Nowadays complex fractionated electrograms (CFAEs) are used to identify areas for catheter ablation, assuming they indicate areas of slow impulse conduction and changes in cardiac tissue structure.
CFAEs last 100 ms and have 8 or more signal deflections.
Fibrosis affects amplitude, duration and the degree of fractionation of signals of electrograms. Increase in density and length of fibrotic strings decreases conduction velocity and increases the amount of fractionation and asymmetry of electrograms. Amplitude is used to distinguish between short and long collagenous strings. It is alway negative, but with a higher negative value in fibrotic tissue.
Electrical mapping methods are based on detection of spatial and temporal distribution of the electrical potential on the cardiac surface. Depolarisation produces a biphasic signal.
Cardiac arrhythmias occur over various spatial and temporal scales and reach from micro re-entry to macro re-entry. At large size scale the excitation can be considered as continuous but at the microscopic level it is complex and discontinuous due to electrical uncoupling by fibrosis. Micro-conduction shows complex pathways in the tissue hardly to detect with conventional systems.
Mapping methods on macroscopic level are based on usage of a large number of electrodes covering the whole heart with the inter-electrode-distance of 1-2 mm. The measured signals are usually digitalised with sampling rates less than 2 kHz. Local activation time is determined as instant of time of peak negative deflection in the first temporal derivate of surface potentials. Such macroscopic mapping systems cannot show all details of excitation wave propagation because of the spatial low -pass effects due to large electrode distances and sizes, and temporal low-pass effects due to the low sampling rates.
These limitations of current electrical mapping systems require further development of more accurate systems to characterise fibrosis on a microscopic size scale.
(30) (35) (36) (37)

Micro-conduction Mapping Method

One possibility to solve these problems is the measurement and analysis of cardiac near field signals. Therefore measurement systems with highest temporal and spatial resolution and ultra-lightweight sensors, floating with the movement of the heart have been developed.

High spatial resolution requirement was solved using sensors with a dense square arrangement of four microelectrodes for measuring unipolar signals Φ which are recorded with respect to a reference electrode considered to be far away from the measurement site.
Sensors are positioned close to tissue surface and the electrical field strength between two opposing electrodes is estimated by a finite differences approach. Amplitude of Φ (Phi pp) can be evaluated from the biphasic depolarization signal.
Spacer pillars are mounted on the tip of sensors allowing non-contact recording without tissue squeezing and preventing lateral slipping. Displacement is also minimised through low mass and flexibility of the sensors.
Through specific configuration of the sensor it is possible to keep SNR under 40 dB and sampling rate higher than 50 kHz.
This method can discriminate between electrical activations with less than 1 mm and 1 ms resolution. The dataset of just four detected signals is not time consuming and allows monitoring in beat to beat manner even at heart rates of 600 beats /min.
Since a spreading excitation wave arrives at the individual electrodes at different instances of time, from the latencies between the local activation times LAT1…4 magnitude of local conduction velocity LCV and direction of wave front propagation φ can be calculated.
LAT's are determined from extracellular signals as the instant of time of maximum negative slope which coincides with the underlying (38)

From the four extracellular potentials Φe1…Φe4 the electrical field strength E (E mag pp) between two diagonal electrode pairs can be calculated by a spatially discrete calculation approach using the diagonal distance DD and the rotation matrix A(α) which considers the orientation of sensor axis and electrode axes (37)

$$\boldsymbol{E} = \begin{bmatrix} \boldsymbol{E_x} \\ \boldsymbol{E_y} \end{bmatrix} = \frac{1}{DD} \boldsymbol{A}(\alpha) \begin{bmatrix} \Phi_{e3}(t) - \Phi_{e2}(t) \\ \Phi_{e4}(t) - \Phi_{e1}(t) \end{bmatrix}$$

$$\boldsymbol{A}(\alpha) = \begin{bmatrix} \cos\alpha & -\sin\alpha \\ \sin\alpha & \cos\alpha \end{bmatrix}$$

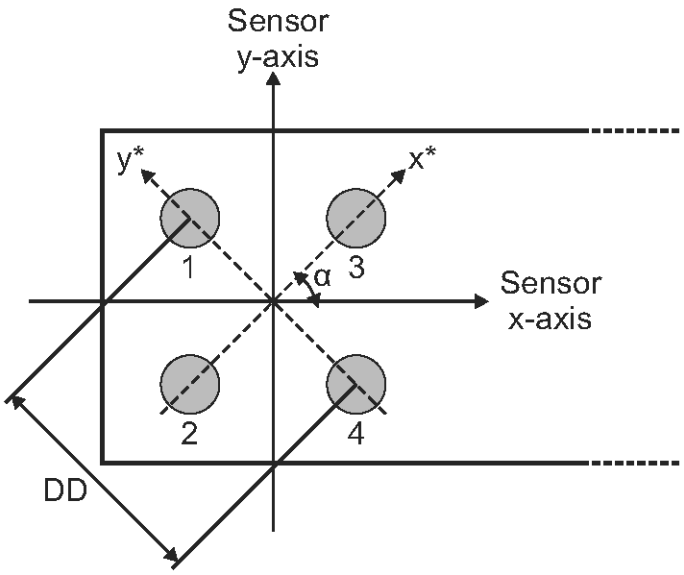

Electrode arrangement and orientation of sensor axes and electrode axes. (Image provided by Dipl.Ing. Robert Arnold, Institute of Biophysics Medical University of Graz)

The resulting components of Ex and Ey can be plotted versus each other.
The resulting vector representation of the cardiac near-field is similar to the vector loops known from vectorcardiography. Morphology of the vector loop of CNF contains information about local properties of activation propagation. Using specific algorithms a fractionation index as a quantitative measurement of fractionation can be computed from extracellular electrograms. (39)

So far the experiments were made on isolated cardiac tissue preparations *in vitro* which differs from perfused preparations or isolated hearts which are three-dimensional and where the boundary of the measurement medium differs. (37) (40) (41) (42) (43)

Right atrium of a rabbit heart with two positioned cardiac close field sensors

Idea: Isolated Hearts in vitro

It is hypothesized, that it might be of importance to test this new micro conduction measurement system in perfused preparations and in isolated Langendorff hearts.
Flexibility, small mass and low dimensions of cardiac near field sensor array make it possible to apply this method on Langendorff perfused isolated hearts of small rodents.

It is to expect that similar findings will be obtained as observed in isolated two-dimensional preparations *in vitro* and computer models that have been developed.
It should be proven that measured surface potentials, electrical near field value, occurrence of fractionation, and conduction velocity changes in correlation with anatomic fibrotic substrates allowing to characterize and quantify them.
The results could be significant for the improvement of intracardial recording at sites not accessible to multi-electrode mapping devices and thus improvement in the diagnosis and therapy of heart fibrosis could be achieved.

Langendorff Preparation

On the basis of experiments on perfused frog hearts by Carl Ludwig's physiological institute in Leipzig, Oscar Langendorff developed the preparation of perfused mammalian hearts in 1897. This led to better insight in heart physiology and myocardial metabolism. Langendorff´s apparatus experienced many modifications over the years but the basics of the concept remained the same.

The heart is perfused mostly with crystalloid perfusion solution. The solution is delivered into the heart over a cannula inserted in ascending aorta. The heart is usually perfused at constant pressure and/or constant flow. Retrograde flow in the aorta closes aortic valve and the entire perfusion solution is directed into the coronary arteries. The perfusion solution flows into the right atrium over the coronary sinus. The ventricle can contract isovolumetrically if an intraventricular balloon is inserted.

The isolated mammalian heart preparation, wide range of physiological parameters, reproducibility and low costs characterise the Langendorff preparation. Together with the fact that animals can be pre-treated with heart potent substances, the Langendorff preparation has emerged to an important and valuable *in vitro* research tool. It enabled the better insight of many physiological mechanisms, including ischemia-reperfusion injury and donor heart preservations. (44) (45) (46) (47)

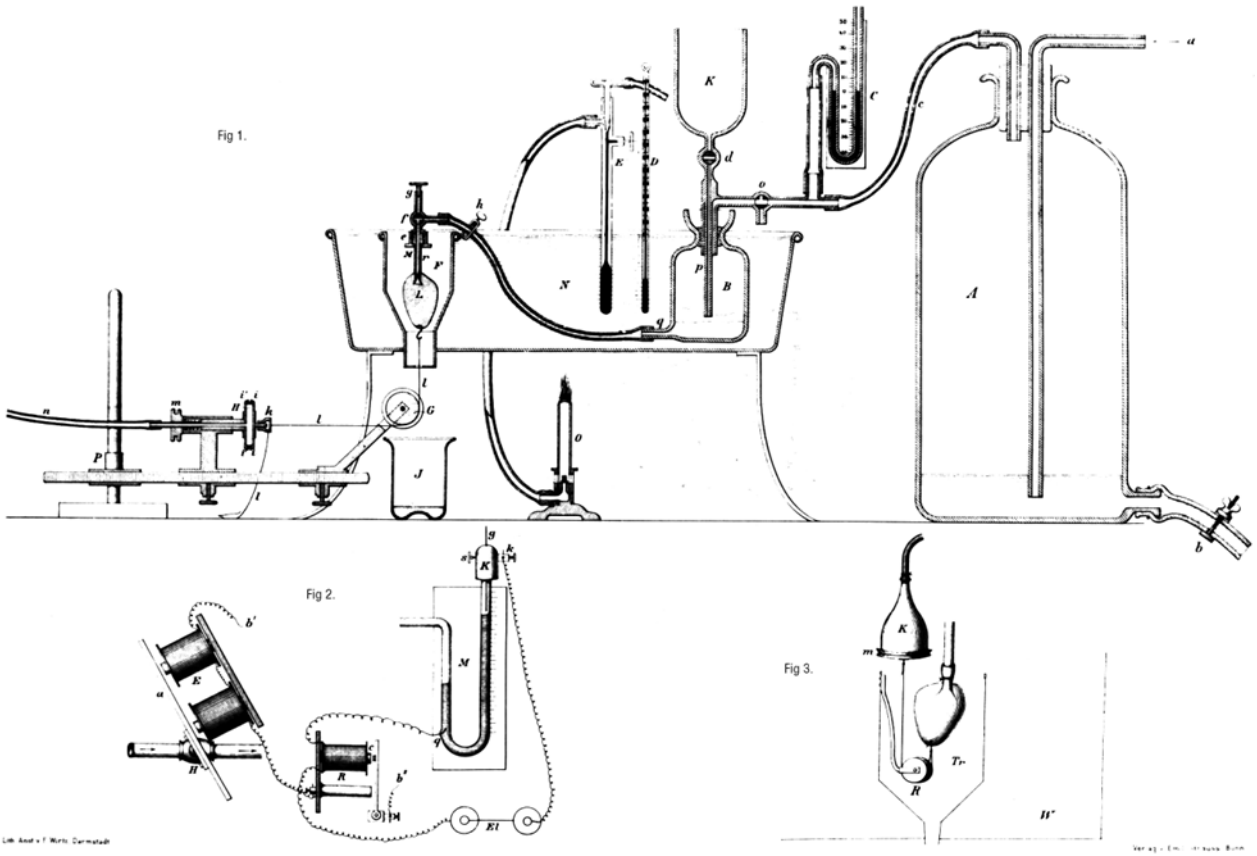

Langendorff, O. Untersuchungen am ueberlebenden Saeugethierherzen. Pfluegers Archiv , (61):291-332, ***1895***

(48)

1. 2 Fibrosis Induction

Different Possibilities

There are different ways of inducing cardiac fibrosis under controlled conditions within preclinical trials.A possibility to induce fibrosis is given through surgical methods another through appliance of pro-fibrotic substances.
There are different molecular pathways that lead to fibrosis induction. The oxidative stress pathway is one in which we can consider the effect of substances with influence on NO synthesis, effects of growth factors or the above mentioned renin angiotensin aldosterone pathway.
As mentioned earlier, some drugs´ (i.e. cyclosporine) adverse effects lead to fibrosis development which was observed in patients´ collectives. Duration and dosage of drug administration were correlated with fibrosis induction and development.
The precise mechanism of the pathway has still not been fully understood, although some relations have been found and described throughout the literature.
As experimental surgical approach, fibrosis can be artificially induced by left descending coronary artery ligation resulting in localised fibrosis i.e. scar formation, or directed to global fibrotic transformation.
The approach of drug application is of importance due to fact that a lot of medications possess these side-effects and might lead, though necessary for certain treatment, to the development of secondary fibrosis. (17) In the field of solid organ transplantation, the use of the well-known IS agent cyclosporine states one outstanding example for adverse development of fibrosis. Testing the impact of CsA on the cardiovascular system is a key topic, not only in the field of solid organ transplantation, but also in the treatment of autoimmune disorders.
This thesis focuses on the verification of the efficiency of micro- conduction measurements of fibrosis induced by cyclosporine treatment.

C62 H111 N 11 O12 = "Simply" Cyclosporine A

The idea of humanity, to transplant organs, has already been implemented as a part of old myths and legends, and can be followed up to the time of 500 BC. The transplant as a surgical invention and its practical realization started in 1880's .In 1950's the patients' immune system was recognized as a key factor to the success of transplantation. A turnover in transplantation surgery was made with discovery of Cyclosporine A in 1971. It was first isolated from extract of the fungus Tolypocladium inflatum gams during screening for novel antibiotics agents and was approved in 1983 for prevention of graft rejection in transplant surgery. One year later a complete chemical synthesis was given. The usage of this agent minimized the repulsion reaction and extended the patients survival time after transplantation. It therefore revolutionized organ transplantation and treatment of immune disorders. It was the first immunosuppressant universally used in allotransplantation and it is still used nowadays. (49) (50) (51) (52)

This molecule has a rather wide spectrum of biological activities, anti-parasitic, fungicidal and anti-inflammatory effects. Nevertheless CsA treatment also shows a number of side-effects on different organs. The reported changes in different organs are dose dependent. So it was shown that a dose of 45 mg /kg body weight in rats resulted in 100% mortality within 2 weeks.

- Renal complications: by acute application of medication glomerulo arteriolar constriction develops leading to a decreased GFR; chronic application leads to RAAS inhibition and activation of profibrotic genes (TGF ß).
- Hypertensive complications have high incidence leading to significant target organ damage
- Cardiotoxicity: occurs in form of increased connective tissue deposition and impairment of vasodilatation by eNOS inactivation (RONS mediated)
- Hepatic complications occur within the first 90 post transplant days
- Neurological complications occur in form from seizures developed through hypomagnesaemia and accumulation of drug metabolites. (53)

Mechanisms of CsA action on fibrosis induction have also been demonstrated.

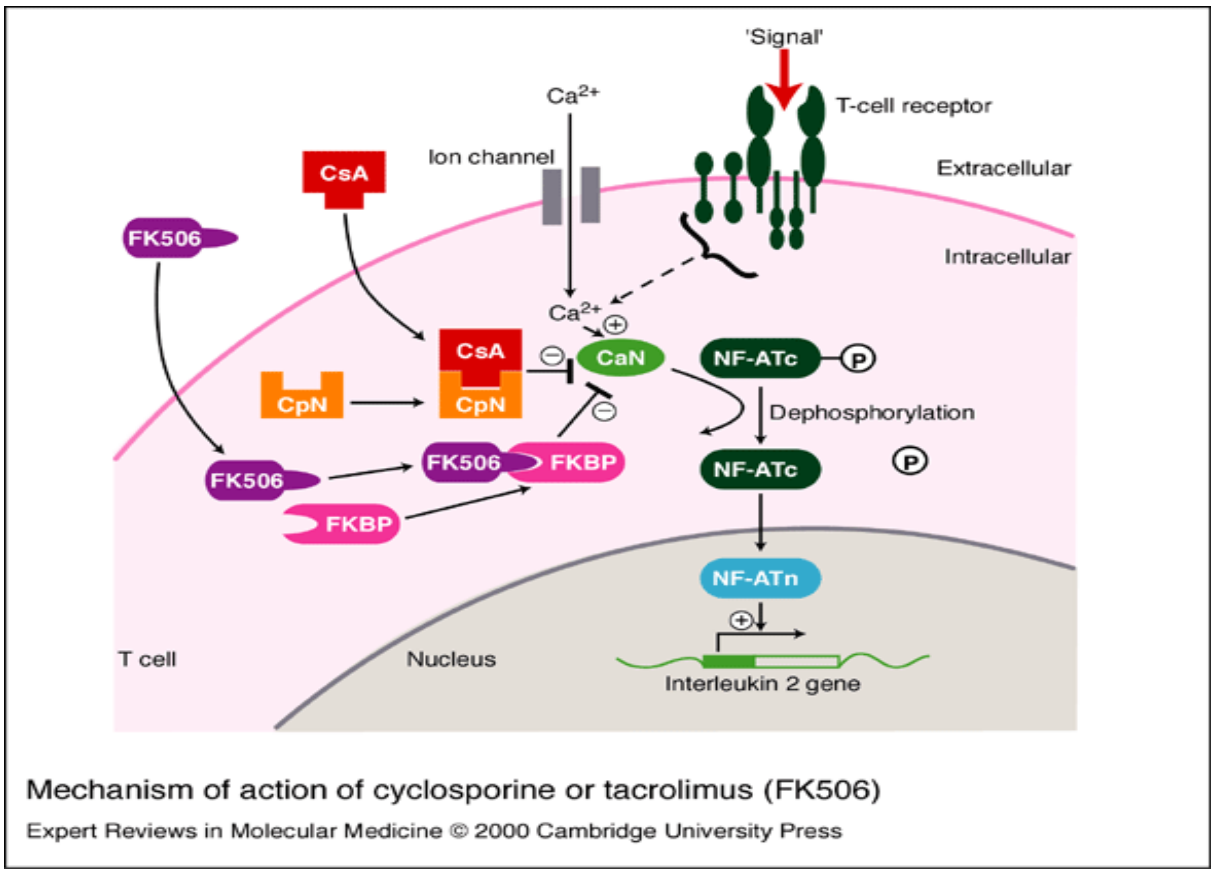

(54)

CsA is associated with a high incidence of hypertension. Patients who develop hypertension, subsequently show left ventricular hypertrophy, lacunar stroke and micro albuminuria. Experimental studies have been undertaken with the aim to show drug effects on the myocardium. CsA has been shown to induce cardio toxicity; involving size, shape and organisation of heart cells in both atria and ventricles. Changes of different proteins of the extracellular matrix where shown. A greater disorganisation of the myofibrillar cytoskeleton was found induced by oxidative damage and apoptosis. (55) (56)

Different stages of damage in cardiac fibres were verified in ultrastructure and the most affected fibres showed modification of the sarcomeres. Bands and myofibrils were rarely recognizable. CsA effects on the cardiovascular system induce a morphological damage through stress protein induction. (57) (58)

Immunohistochemical methods proved an increase in iNOS, in vascular endothelial growth factor, heat shock protein and matrix metalloproteinase.

Small heat shock proteins (sHSPs) stabilise the cytoskeleton and protect its components from toxic and ischemic factors inside the myocardium.

Prolonged treatment with cyclosporine affects the distribution and solubility of small heat shock proteins and alpha B crystalline in rat hearts .This might be an endogenous reaction to compensate CsA damage. (17) (59)

Several studies showed that cyclosporine effects ionic channel activities in human cells.

It is not clear if CsA affects the ion channels dependent or independent of the calcineurin mechanism.

In ventricle myocytes, an inhibition of K^+ channels was detected causing a long QT syndrome. K^+ channels are subdivided in slow and rapidly activating components. The rapidly component was encoded to belong to the hERG gene and mutation of the same is resulting in a long QT syndrome which has been related to tachyarrhythmia and potentially sudden cardiac death.

It was also shown that drugs which block hERG channels cause cardio toxicity. CsA was proven to inhibit the cloned hERG channels in human cell lines. Some results suggest that CsA directly blocks hERG channels in a calcineurin independent manner. It can be presumed that most likely CsA causes cardio toxicity via a prolonged QT time resulting in ventricular tachyarrhythmia. (60)

In contrary, protective effects of cyclosporine are also described in some studies. Coronary artery ischemia reperfusion injury occurs by restoration of coronary flow after a period of myocardial ischemia and includes myocardial cell injury and necrosis, followed by fibrosis. Apoptosis is the primary cause of cell death in this setting. Hereby injuries of the mitrochondria occur.

Cyclosporine A is a potent inhibitor of mitochondrial permeability transition pore -MPTP opening and has been shown to protect isolated cardiac cells against reperfusion injury. Pre-treatment with CsA in ischemia-reperfusion prohibits the injury of myocytes. This suggests that CsA on this way might reduce ischemia induced damage.
CsA effects are not specific and CsA also inhibits calcineurin, which as well plays an important role in modulating mitochondrial injury. Inhibition of caspasis activity can be associated with this mechanism too. (61)

2) OBJECTIVES

Our first aim was to prove that fibrosis, induced by CsA administration, can be detected and quantified via the cardiac near field mapping through the presence of impaired signals.
The second objective was to correlate these signals with the anatomic fibrotic substrate.

3) MATERIALS AND METHODS

3. 1 Animals

In contrary to clinical studies animal models hold a full access to tissues and all variables that might confound the outcome can be fully controlled. Therefore these models are widely used to explore hypothesis in advance to human studies.
The changes in rat kidneys and rat hearts were shown to be strongly similar and comparable to those in human – therefore studies on rat myocardium provide a perfect example for human myocardium.
The present study focuses on a new method for mapping of electrical conduction disorders in isolated rat hearts.
Furthermore, cardiac function and coronary flow were evaluated using the Langndorff technique. (62) (63) (64)
The whole study was designed, using the three R's as basis, which refers to replacement, reduction and refinement. Animals cannot be replaced. Sample size calculation yield that four animals in the control group and six in the treatment group were sufficient to achieve statistically significance. During experiments, care was taken to minimize distress. This was achieved by calm and proper handling of the experimental animals. To prevent unnecessary pain, analgesia and anaesthesia according to the latest guidelines were used. (65) (66)

The present study was approved by the ethic committee (BMWF= Bundesministerium für Wissenschaft und Forschung, BMWF-66.010/0068-II/3b/2011).

The animals were divided into two groups according to received treatment:

CsA group: 6 male Sprague Dawley rats (Tierversuchsanstalt Himberg , Vienna) (250-300 g) were subjected to a daily intraperitoneal Cyclosporine A injection in a dose of 15 mg/kg KG for 45 days, as reported by previous studies to induce chronic kidney failure and heart fibrosis.
Standard rat chow and water were accessible *ad libitum.*
They were housed under constant temperature and exposed to a 12 h day and night cycle.

Control group: 4 male Sprague Dawley rats (Tierversuchsanstalt Himberg ,Vienna) (250-300g) were subjected to daily intraperitoneal olive oil (vehicle for CsA) injections for 45 days.
Standard rat chow and water were accessible *ad libitum.*
They were housed under constant temperature and exposed to a 12 h day and night cycle.

3. 2 Materials

3.2.1 Materials and Medication

Pre-treatment medication:

Olive oil		(Commercial olive oil)
Sandimun ® (Cyclosporine):	15 mg /kg/BW/day	(NOVARTIS) i.p.

Salts for perfusion solution (Krebs Ringer solution):

Aquabidest	(Fresenius Kabi Austria GmbH)
NaCl	(Carl Roth GmbH)
KCl	(Carl Roth GmbH)
KH2PO4	(Carl Roth GmbH)
MgSO4 7H2O	(Carl Roth GmbH)
CaCl2 2H2O	(Carl Roth GmbH)
NaHCO3	(Carl Roth GmbH)
Dextrose [D-glucose]	(Carl Roth GmbH)

Drugs for anaesthesia:

Ketosol ® (Ketamin) :	75mg/kg BW	(GRAEUB)
Heparin Immuno ® 1000 IE /ml:	400 IE i.p.	(EBENE)
Gewacalm®5mg/ml (Diazepam):	2,5mg/kg BW	(NYCOMED)

Tissue conservation:

4% Formaldehyd (Donau Chem Gmbh)

Filter system: Millipore Express plus, Φ 0.22 µm

Centrifuge: ABBOTT, serial number 182860

Camera: LEITZ (Nr 543629)

Microscope: WILD-HEERBRUGG, M-400 Photomacroscope

Laboratory glassware, magnetic stirrer were used from the Langendorff laboratory of the Section of Surgical Research as well as surgical instruments, syringes and needles.

3.2.2 Perfusion Solution

Langendorff perfusion solution recipe:

Stock solution:

1000 ml stock solution:
Aqua bidest
138, 4 g NaCl
7, 0 g KCl
3, 2 g KH2PO4
5, 8 g MgSO4 7H2O
7,4g CaCl2 2H2O

Recipe:

In 700 ml Aqua bidest a magnetic stir bar was added. The salts were added in precisely same order as previously listed. Only when the previous salt was completely solved the next one was added.

CaCl2 2H2O was diluted solitary in 50 ml Aqua bidest and stirred till the solution became transparent. Thereafter it was added to the solution.
The stock solution was then stored in a light protected glass container and stored in the fridge at 4°Celsius.
It had to be used within one week.

Krebs Ringer Solution (KRS):

For 2000 ml use:
100 ml Stock solution
+1900 ml Aqua bidest
+4, 4 g NaHCO3
+4, 2 g Dextrose [D-glucose]

Recipe:

At first 500 ml Aqua bidest had to be filled in a 2L Erlenmeyer flask and 4,4g NaHCO3 was added. The solution was shaken until the salt was completely solved.
Then 4,2g Dextrose was added and proceeded the same way. At the end 100 ml of stock solution and 1400ml of Aqua bidest were added.
Thereafter the solution had to be filtered and warmed in the waterbath at a constant temperature of 38°Celsius.
The mixed Krebs Ringer solution had to be used within one day.

3.2.3 Perfusion System

Langendorff apparatus (Hugo Sachs Harvard Apparatus GmbH):

Langendorff -Isolated Heart for Small Rodents IHSR

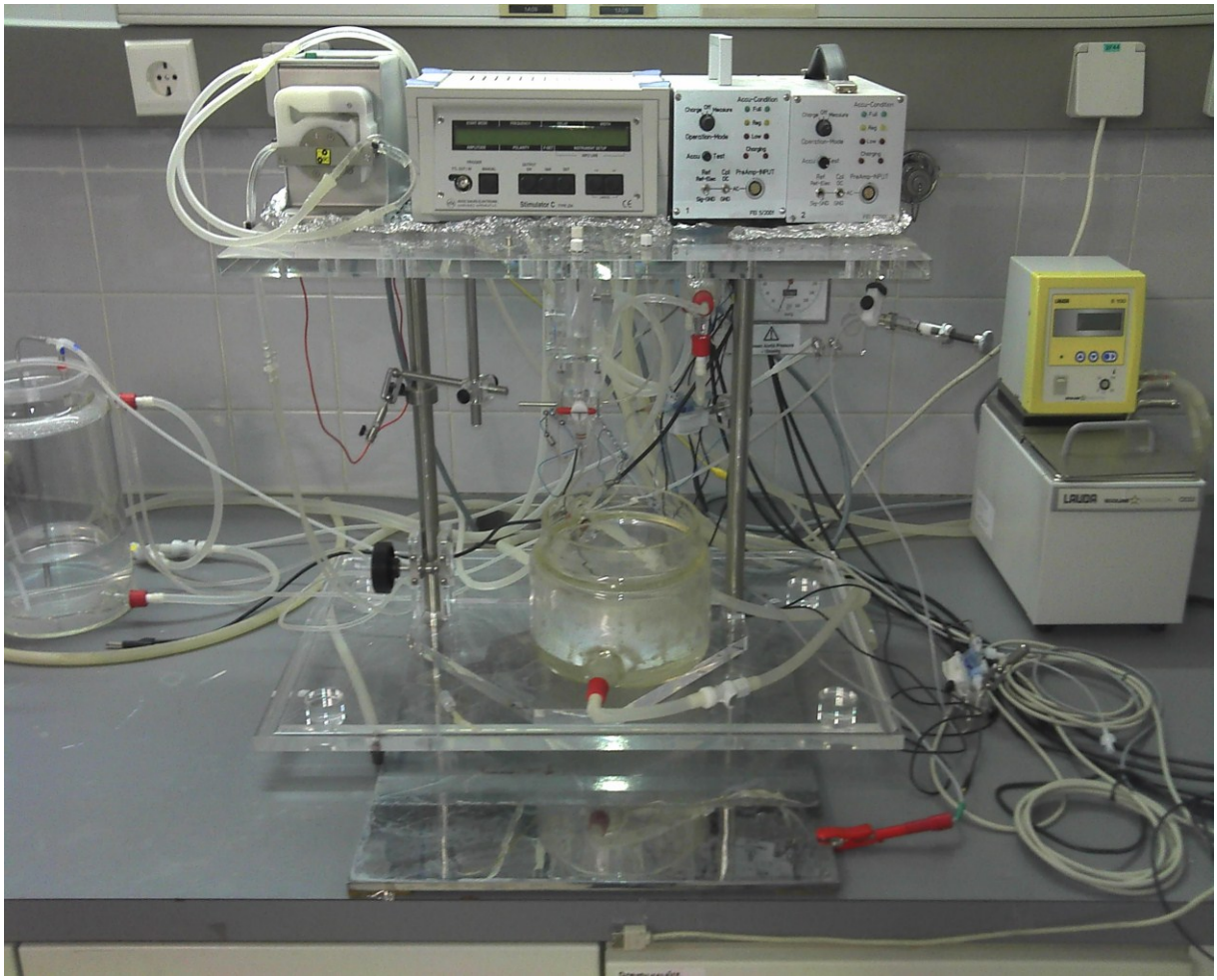

Langendorff was the first one who described the isolated retrograde perfused mammalian heart preparation. The basis of the concept stayed the same throughout the years. Blood or crystalloid perfusion solution is delivered to the rat heart over ascending aorta cannula. Retrograde flow makes the perfusion solution drain the coronary vessels and flow into the right atrium.

Parts of the Langendorff Apparatus

- Reservoir for the perfusion solution,
- Warm water reservoir attached to a pump that supplies water jackets around the bulk perfusate reservoir,
- Heart chamber and the chamber for the oxygenated perfusate,
- Pump to deliver the perfusion solution to the oxygenator,
- An overflow to maintain the constant level in a perfusate reservoir,
- Graduated container to measure the coronary flow from right atrium to the coronary sinus
- Appropriate taps for measurement of pressure and flow transducers are included
- A balloon attached to pressure transducers should be placed in the left ventricle to monitor left ventricular pressure and its derivations and to control preload
- Physiology data acquisition systems
- Signal conditioners for conversion of physiological signals
- Transducers for data transduction

(67)

3.2.4 Cardiac Near Field Measurement System

CNF Sensors:

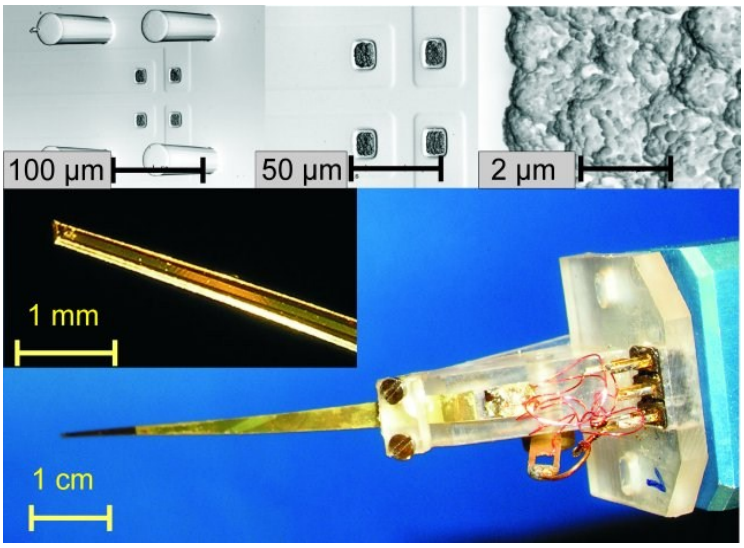

The fabricated near field sensor taken at different scales: the photograph shows sensor tip, carrier and connector to preamplifier, the electron micrographs electrodes, leads and spacers.
(A new floating sensor array to detect electric near fields of beating heart preparations, E. Hofer, F. Keplinger, T. Thurner, T. Wiener, D. Sanchez-Quintana, V. Climent and G. Plank ; Biosensors and Bioelectronics;(21); 2006)

For characterization of local spread of electrical activation low-mass, flexible miniature sensor was custom-designed. This sensor is made of polyimide making it flexible enough to follow the contraction movement of the heart. Spacer pillars at the sensors' tip maintain constant sensor-tissue spacing of 70 µm for non-contact measurements. At the tip of the sensor 4 Ag/AgCL electrodes are mounted in a quadratic arrangement with 50 µm interelectrode spacing. Unipolar extracellular electrograms Φe are measured with respect to a reference electrode considered to be "far away" from the measuring site.

The sensors are mounted on 3D micromanipulators allowing arbitrary positioning of the sensors.

Measurement System:

Extracellular recordings Φ_e are amplified by a factor of 100, analog filtered (4^{th}-order Bessel, -3dB-point at 25 kHz), and digitized with a sampling rate of 100 kHz per channel (NI-9215, National Instruments, Austin, Texas).

Data acquisition and data storage is controlled via a custom-designed software application written in LabVIEW (National Instruments, Austin, Texas) and running on a standard laptop PC (Dell Latitude E6500).

Documentation of consecutive measurement sites is done with a digital camera (Olympus C-5060 WZ, Olympus, Japan).

(41)

3. 3 Methods

3.3.1 Study Protocol

The rats were divided into two groups, mentioned above, 4 rats were assigned to the control group and 6 rats to the CsA treated group.
All rats received a low-sodium diet, food intake was ad libitum. Water intake was restricted to 35 ml daily. (Average daily water intake of male Sprague Dawley rat can be estimated with 30 ml).
Body weight was monitored weekly.
On day 0, 7, 14, 21, 28, 35, and 42 of treatment, blood samples were taken from every animal to measure CsA levels.
The blood was withdrawn from the lateral tail vein through venipuncture using a 24 gauge needle. A maximum of 1 ml blood can be taken once according to a general guideline as not more than 10 % of the circulating blood volume may be collected in order to avoid hypovolemia. This limits the amount of parameters for examination. For the present study soley the CsA levels were determined. According to the guidelines of the Animal Care Services, no anaesthesia is needed to obtain blood from the tail vein.
Five to fifteen minutes prior to venipuncture, the animals were warmed with a low-wattage light to ensure maximum vasodilatation of the veins. Then the rats were restrained through a mechanical device. The area of injection was cleaned with alcohol, if necessary blood pooling was induced by placing a small rubber band around the base of the tail. Afterwards venipuncture was performed.
Blood was withdrawn, serum was obtained through centrifugation at 10.000 rpm for ten minutes and stored for further biochemical investigations at -20° Celsius.
On day 45 the animals were sacrificed and the hearts were attached to the Langendorff system. (see below)

3.3.2 Experimental Protocol

The body weight of each rat was weighed prior to the scarification.
Ten to 15 minutes after intraperitoneal injection of 75 -100 mg/kg BW Ketamine, Diazepam 2,5 mg/kg BW and 400 IU of Heparin, the depth and analgesia of the anaesthesia was checked by the animals' response to a toe pinch. (66) (68) (69).
Only if the animal was not responding to the pinch, the surgical procedure was started.
Laparotomy was performed to get access to the abdominal aorta for the final blood sampling.
Right after, thoracotomy was performed and the heart was rapidly separated from its neighbouring structures and finally explanted. (67)
Through a 1.0 ± 0.3 cm aortic stump the heart was attached to the Langendorff apparatus and perfused with Krebs Ringer Solution (KRS).
The perfusion fluid was maintained at 37 ± 1 °C, with a pressure of 70 mmHg and constant oxygenation (5 % CO_2/ 95 % O_2).

The Langendorff system records mechanical parameters and cardiac rhythm of the working myocardium.
Left ventricular ejection fraction i.e. the correlation of the end diastolic volume and the stroke volume and the thickness of the chamber or the atrial wall were measured in order to estimate the left ventricular function as well as atrial contractile force and filling pressures. These parameters also reflect the amount of fibrosis.

An indirect measurement of atrial force is possible through measurement of left atrial ejection fraction; another way would be by measuring the flow velocity due to atrial contraction.
In case of atrial fibrillation caused by fibrosis the left ventricular compliance and reservoir function –i.e. the left ventricular function are impaired, due to the fact that there is only the passive force for ejection fraction and thereby the contractile force and flow should show significant differences in fibrotic arrhythmic tissue. (13) (22) (70) (71) (72)

The coronary flow was measured by the collection of the perfusate over a period of 1 minute at regular intervals. Via a force transducer the contractile force (tension, ***g***) as well as the diastolic tension were recorded. Electrical activity was recorded using ECG electrodes that were placed directly on the surface of the right atrium and left ventricle (bipolar lead).

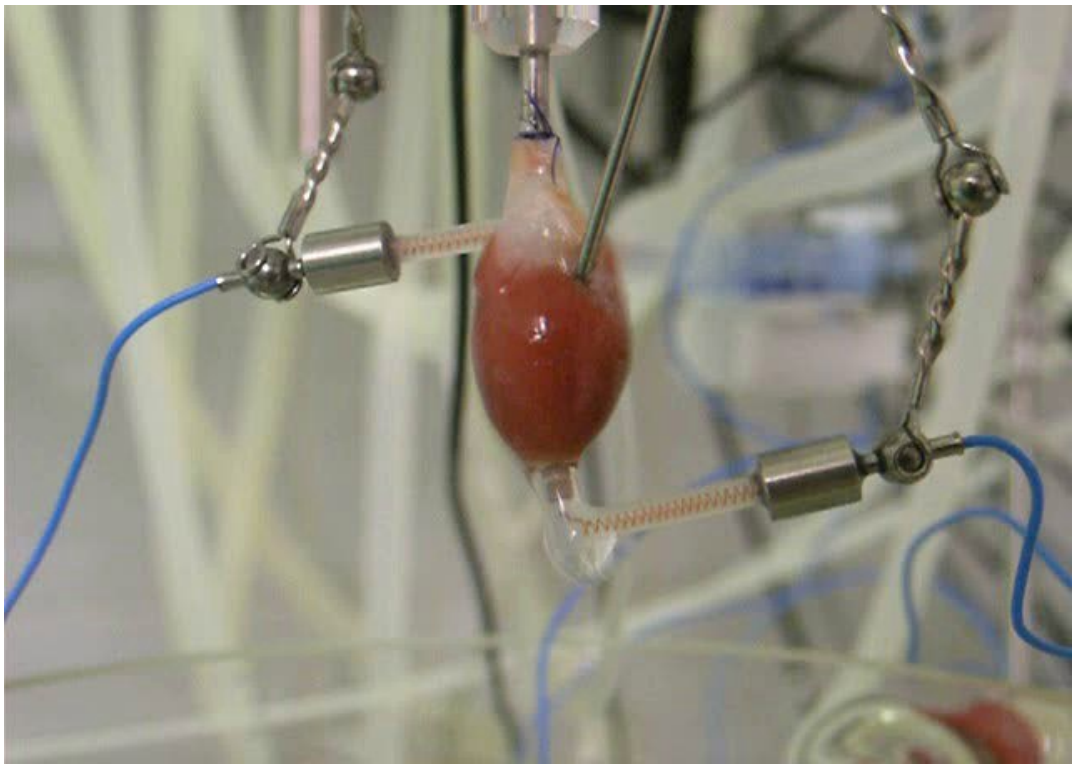

The physiological performance of the hearts of the two groups was measured via this technique using following protocol:
15 minutes stabilization,
30 minutes baseline
15 minutes occlusion, the ligature of LAD was performed
30 minutes of reperfusion

The apex of the heart was fixated immediately for histological processing and the heart basis was frozen on -80°C for biochemical analysis.
The occlusion/reperfusion protocol was used to determine possible differences in the occurrence and the duration of post-ischemic arrhythmias.
In addition to the above mentioned measurements, a flexible micro-sensor containing four recording Ag/AgCl electrodes was placed in the cardiac electric near field close to the surface of the beating heart.
Right after the experiment and before harvesting and storing the heart for further investigations it was weighed.

3.3.3 Micro-conduction mapping

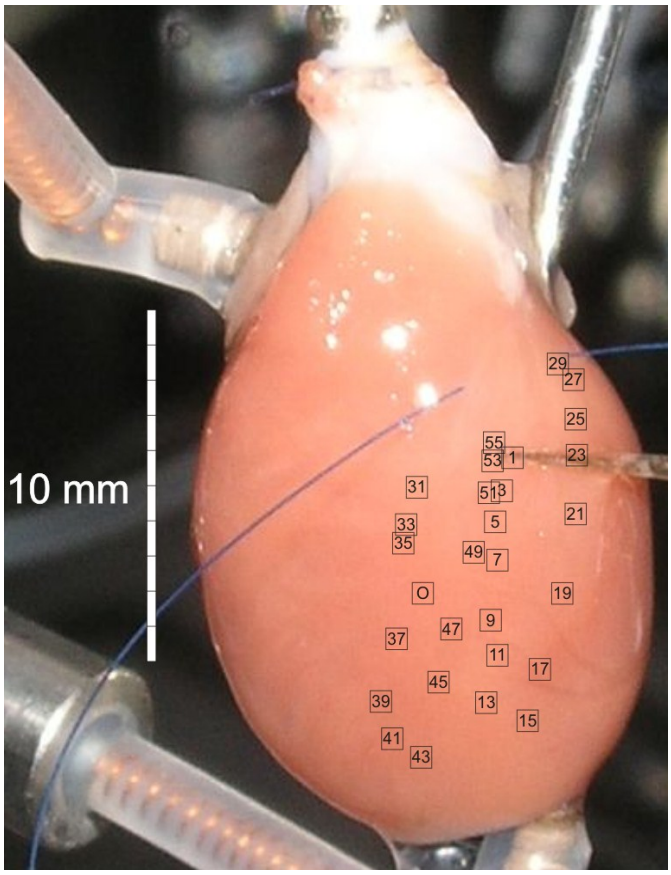

Image of exemplary experiment with measurement positions in black rectangles

After stabilization of the hearts on the Langendorff apparatus, electric near-field measurements were started. Sequential mapping of the epicardial left ventricle was performed by consecutively moving the sensor to a measurement site, taking an image of the current position, and recording at least 2 heart beats.

CNF data together with ECG recordings and left ventricular pressure data were saved on hard disk for later off-line analysis.

Different electrical field measurements were performed. Those included into the present analysis were:

$\Phi_e(t)$: peak-to-peak voltage of the extracellular potential Φ(mV)

$d\Phi_e(t)/dt$:max negative peak voltage (from zero to the negative maximum) in the first temporal deviation of the extracellular potential Φ(V/s)

FI fractionation index: number of deflections in $d\Phi/dt$

The measurement system only detects a peak if the peaks size is above 10% of the experienced maximum peak.

FI = 1 unfractionated

FI= 2 middle fractionated

FI≥3 high fractionated

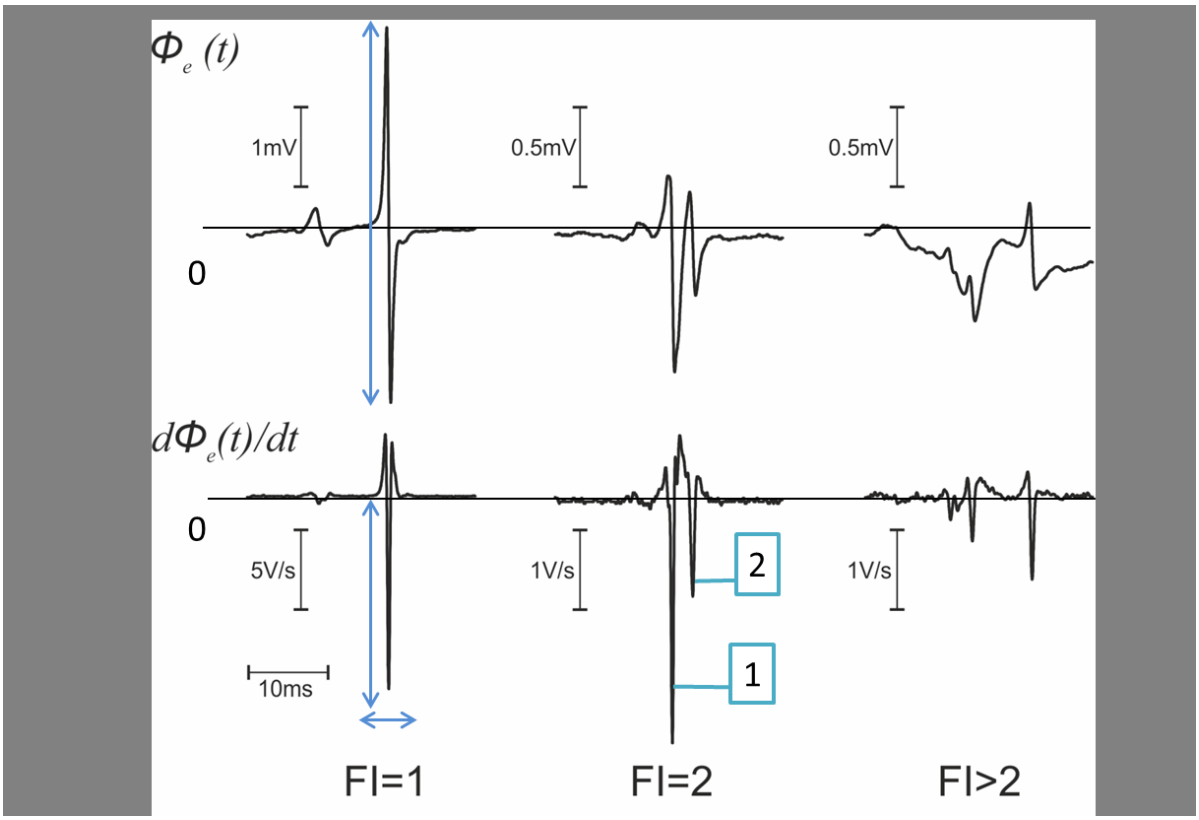

The following electrical field values were measured and calculated:

With the micro conduction sensor four surface potentials $\Phi_e(t)$ were measured and recorded. Respectively two of them were merged and interpolated resulting in Ex(V/s) and the other two resulting in Ey(V/s).

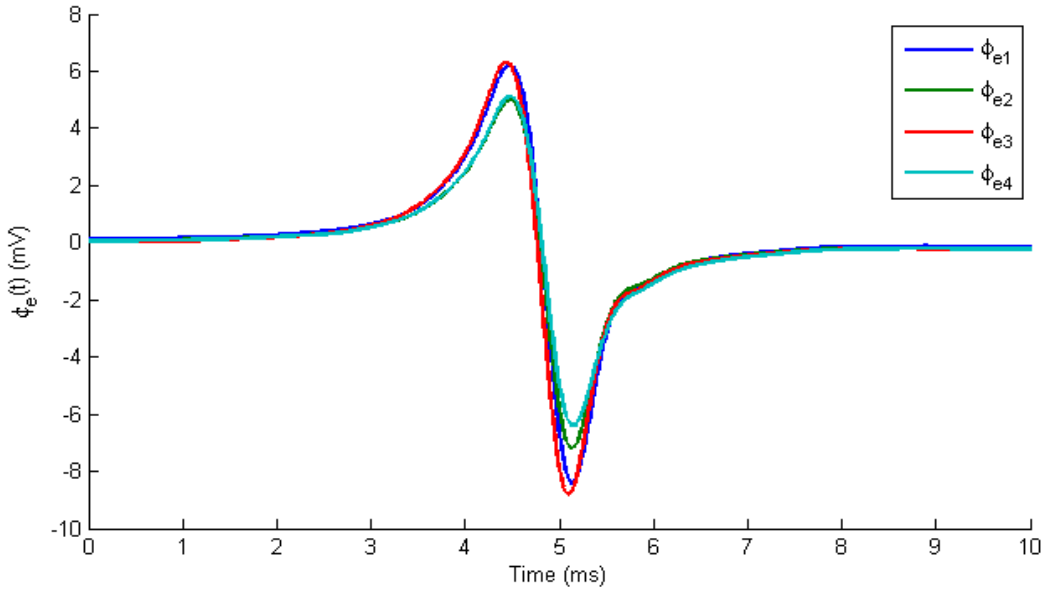

Four electrical potentials measured with four electrodes of the sensor

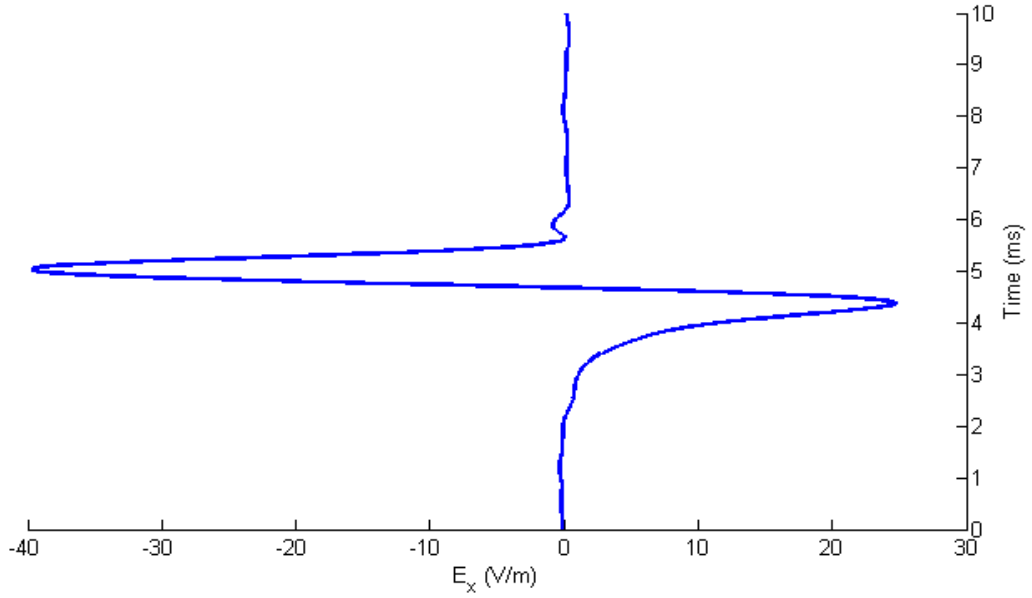

Ex interpolated E value of pair of two merged electrodes

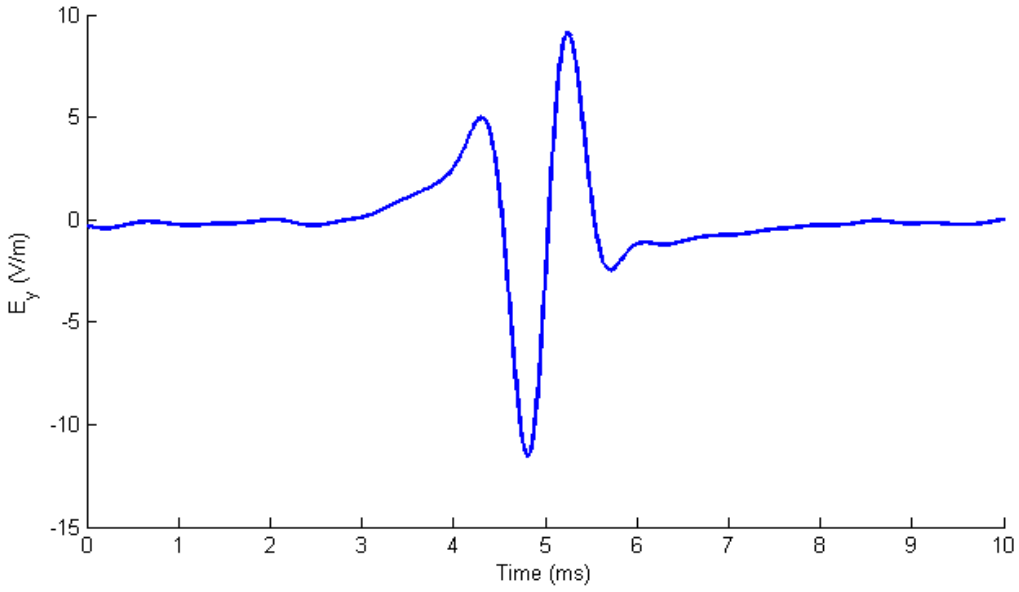

Ey interpolated E value of pair of other two merged electrodes

From this measured and interpolated values through further interpolation of Ex and Ey values a vector loop of E was calculated. E represents the cardiac near field strength. The vector describing the vector loop origins in the point 0x0y and moves clockwise along the vector loop. The position in which the vector value takes the largest magnitude (the maximum longitude of the vector) is called the Emax for value of E, as a maximum magnitude of cardiac near field strength. (41) (42)

Emag : maximum derived magnitude of cardiac near field strength (V/m)

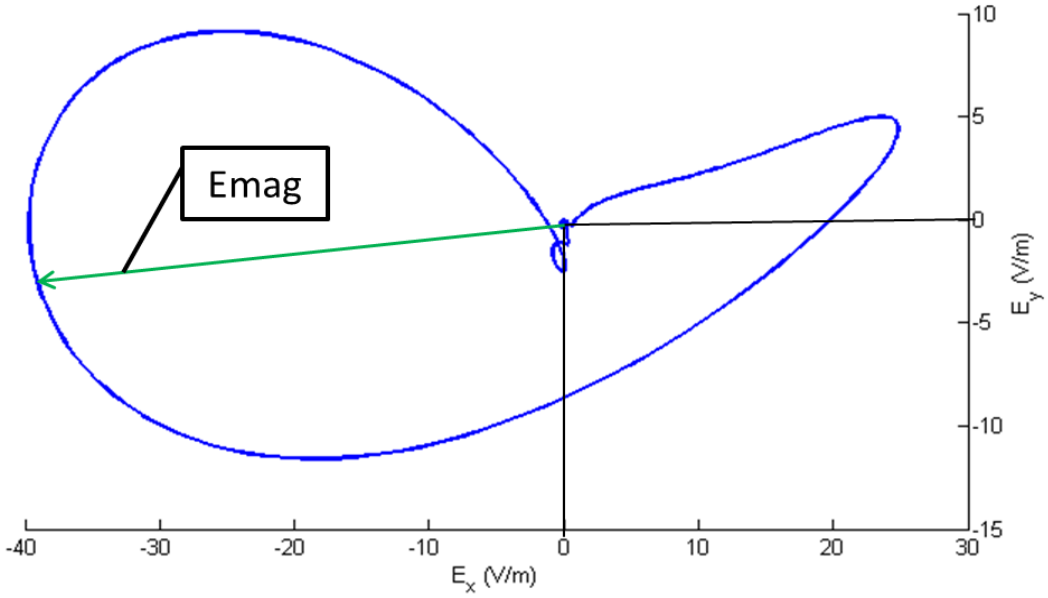

3.3.4 Physiological Data

For the assessment of mechanical function, diastolic compliance and chamber stiffness peak LV developed pressure (LVpdP) ,coronary flow and heart rate were recorded continuously.
The heart weight was measured on the scarification day body weight was measured once a week during the whole study period and on scarification day as well.

3.3.5 Statistical methods

All data are presented as median and standard deviation unless otherwise indicated. All data were checked for normality using the Kolmogorov-Smirnov test. All data were equally distributed. To test the inter group equal variance the Levene`s test was used. Once normality demonstrated, for between group comparisons, unpaired Student`s t-test was used. The changes in the parameters compared to baseline were also analysed using the Student`s t-test. All statistical analyses were performed using SPSS 19.0 (IBM, Chicago, IL, USA) and a $p < 0.05$ was considered significant.

3.3.6 Histological Stains

Beyond 90 minutes of measurements on the Langendorff apparatus the heart apex was cut off , washed in saline and then fixated immediately for histological processing. Each heart was fixed with 4% polyformaldehyde . Fixed-sections were dehydrated and embedded in paraffin. Afterwards the heart apex was sectioned into 4 sections, each section was divided into a 5-µm thick slices. One representative slice per section was subjected to haematoxylin–eosin (HE) and Masson's trichrome stain to show tissue fibrosis.

Masson's Trichrome Staining Protocol for Collagen Fibres was used for the detection of collagen fibres in the included rat hearts. The collagen fibres were stained blue and the background appears stained red.

Haematoxylin and Eosin (HE) Staining showed indicator-like properties, by being blue and less soluble in aqueous alkaline conditions, and red and more soluble in alcoholic acidic conditions. In the heart the collagen fibres would be stained pale pink while the surrounding muscle will be in deep pink colour. (73) (74) (75)

Histomorphometric analysis was performed by using a light microscope with x250 magnification. The tissue was evaluated semi-quantitatively by randomly selecting at least three fields of each slice. Histopathological findings of fibrosis were evaluated. Papillary muscles were excluded from the fibrosis measurement. Particular attention was paid to the exclusion of fixation artefacts, blood vessels and endocardial plaque from the analysis. Due to the fact that the extent of fibrosis was not homogeneous it might not be representative for the whole slice. A single investigator unaware of the experimental groups performed the analysis.

Each layer was graded percentually to give the histopathological score.

4) RESULTS

4. 1 Characteristics

The rats were randomly included into the CsA treated group (n=6) or the control group (n=4) The number of n=4 in control group was considered as high enough due to the fact that this group wasn't expected to undergo any changes during the study . One rat out of the control group suffered an arrhythmia at the beginning of the experiment therefore this animal was excluded from further analysis (n=3).

Body weight was measured during the study as well as heart weight which was measured on the day of sacrification. CsA blood levels were estimated continuously including on the scarification day. From weekly CsA levels a mean CsA level per rat, at the end of the study was estimated. Differences in CsA levels among the rats in the CsA treated group were observed. However these differences were not statistically significant (p=0.09).

Table 1:

Rat	Mean per rat [µg/mL]	Rat	Mean per rat [µg/mL]
I	3,5	IV	2,68
II	2,92	V	2,26
III	1,87	VI	3,43

Differences in CsA levels among the rats in the CsA treated group were observed. However these differences were not statistically significant (p=0.09).

The mean CsA blood level in the whole group was: 2, 78 µg/mL, with a standard deviation of 0,64.

The mean dosage in CsA for each rat was over 1,5µg/mL blood taken.

These data confirm that CsA blood levels were achieved in an effective dosage through levels of 100-200 ng/ml. (76)

Table 2:

Measurements	Mean CsA group	Mean control group	Standard deviation CsA group	Standard deviation control group	P value
Body weight (g)	330,263	371,650	36,6312	58,2631	0,111
Heart weight (g)	1,3917	1,6667	0,28708	0,05774	0,156

As shown in table both groups did not differ in terms of body weight or heart weight.

Physiological Measurements

During the whole experiment, each animal's heart rate, left ventricular peak diastolic pressure and coronary flow were continuously recorded. Results gained every 5 minutes were included into the statistical analysis – therefore 21 measurements were included in each group.

Table 3:

Measurements	Mean CsA group	Mean control group	Standard deviation CsA group	Standard deviation control group	P value
Coronary flow (ml/min)	7,6343	7,0090	0,52347	0,98195	0,014*
Heart rate (bpm)	257,7967	192,5524	31,17860	55,66887	0,0001
LVpdP (mmHg)	63,6801	61,4393	15,86277	21,13800	0,700

** Due to large deviations from normal distribution, t- test not convincing*

As shown in table both groups did not differ in terms of coronary flow and LVpdP. The groups significantly differ only in magnitude of the heart rate.

Histological Analysis

Histological analysis was performed to detect fibrosis and estimate the extent of an existing fibrosis.

The Utah classification of fibrosis was used to determine the extent of fibrosis histopathologically. According to this classification there are 4 categories of fibrosis. The classification depends on the percentage of fibrosis:

1°: <5% minimal

2°: >5–20% mild

3° : >20–35% moderate

4°: >35% extensive

Electrophysiological Measurements

Electric near-field measurements and a sequential mapping of the epicardial left ventricle were performed. The sensor was consecutively moved to a measurement site and at least 2 heart beats were recorded. In total 155 measurement points were measured into the CsA group and 77 in the control group for each measured value.

Table 4:

Measurements	Mean CsA group	Mean control group	Standard deviation CsA group	Standard deviation control group	P value
$\Phi_e(t)$ (mV)	11,6773	12,7576	3,42334	3,71148	0,29
$d\Phi_e(t)/dt$ (V/s)	24,5096	18,6823	14,51077	11,11458	0,002
Emag (V/m)	26,7708	30,7173	15,61710	16,86156	0,79
FI	1,25	1,57	0,491	0,677	0,0001

As shown in table both groups differ in terms of $\Phi_e(t)$ (mV), $d\Phi_e(t)/dt$ (V/s) and FI ; but there is no significant difference in magnitude of Emag.

4. 2 Results of Physiological Measurements

Body weight

Once per week in addition to scarification day, in total 8 measurements of body weight were performed within both groups. The included data were not normally distributed. (p = 0,132 (CsA group) and p = 0,200 (control group).
Nevertheless the comparison of mean values for CsA and control group showed that the mean body weight throughout the study was smaller in the CsA group (330,263g) than in the control group (371,650g).

Heart weight

On scarification day, after the Langendorff experiment, the heart of each animal was weighed.. In total 3 hearts were weighed in the CsA and 6 hearts in the control group. Although the included data were not normally distributed (p = 200 as a lower bound of the true significance) a mean heart weight of both groups differed significantly (CsA = 1,3917g, control group = 1,6667g). This indicates that the gain in heart weight was higher in the control group compared to the CsA group.

LVpdP

In total 21 LVpdP were measured within the CsA group and the control group. The results showed too large deviations from the normal distribution (p= 200 for both groups) and therefore the data and t- test were not convincing.

Coronary flow

The coronary flow was measured every 5 minutes. In total 21 coronary flow measurements for each group were performed. It was demonstrated, that the data were not normally distributed, particularly the CsA group showed a large deviation (p= 0,114) whereas the control group showed a similar deviation (p=0,051) from the distribution.

Heart Rate

In total 21 heart rate measurements in the CsA group and in the control group were performed. The data using the Kolmogorov Smirnov test were normally distributed for both groups ($p<0,05$ ($p= 0,012$ CsA group), ($p= 0,004$ control group). In addition the Levene's test of equality of variances was made showing that variances were homogeneous by insignificant $p> 0, 05$ ($p>0,092$). Thereby the criteria for t- test performance were fulfilled.
T-test showed that there was a significant difference in HR between CsA and control group $p<0,05$ ($p=0.000 < 0.05$).
The CsA treated group showed higher values of heart rate in comparison with control group during the experiment. The mean of heart rate for the CsA treated group was higher (257, 7967 bpm) than in the control group (192, 5524 bpm).

Graph 1:

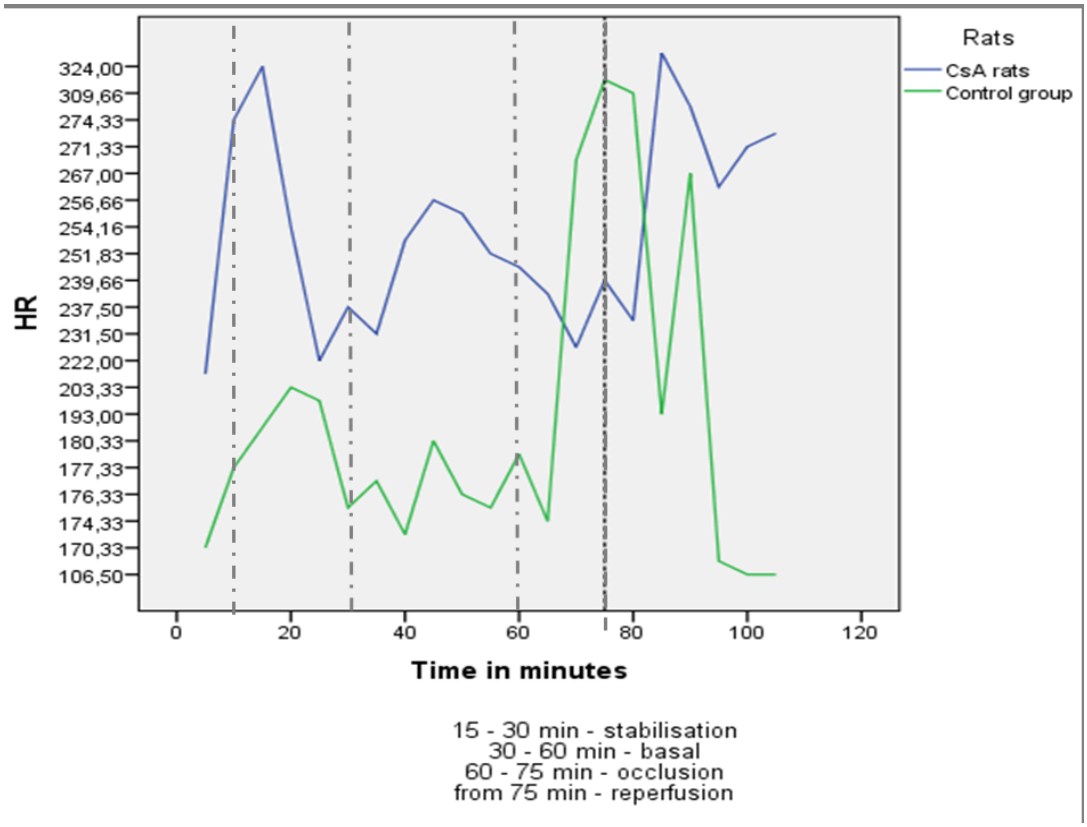

The graphical presentation of heart rate during experiment (implicating the periods of stabilisation, basal period, occlusion and reperfusion period)

We wanted to compare data for the reperfusion period alone, with the aim to show if there was a difference between study groups in occurrence of higher percentage of arrhythmia and fibrillation in this period, induced by occlusion of LAD . The Kolmogorov Smirnov test of normality showed that the results were not interpretable because of too large deviation from the normal distribution. Therefore the performance of t- test was not possible.

4. 3 Interpretation of Electrical Near Field Measurements

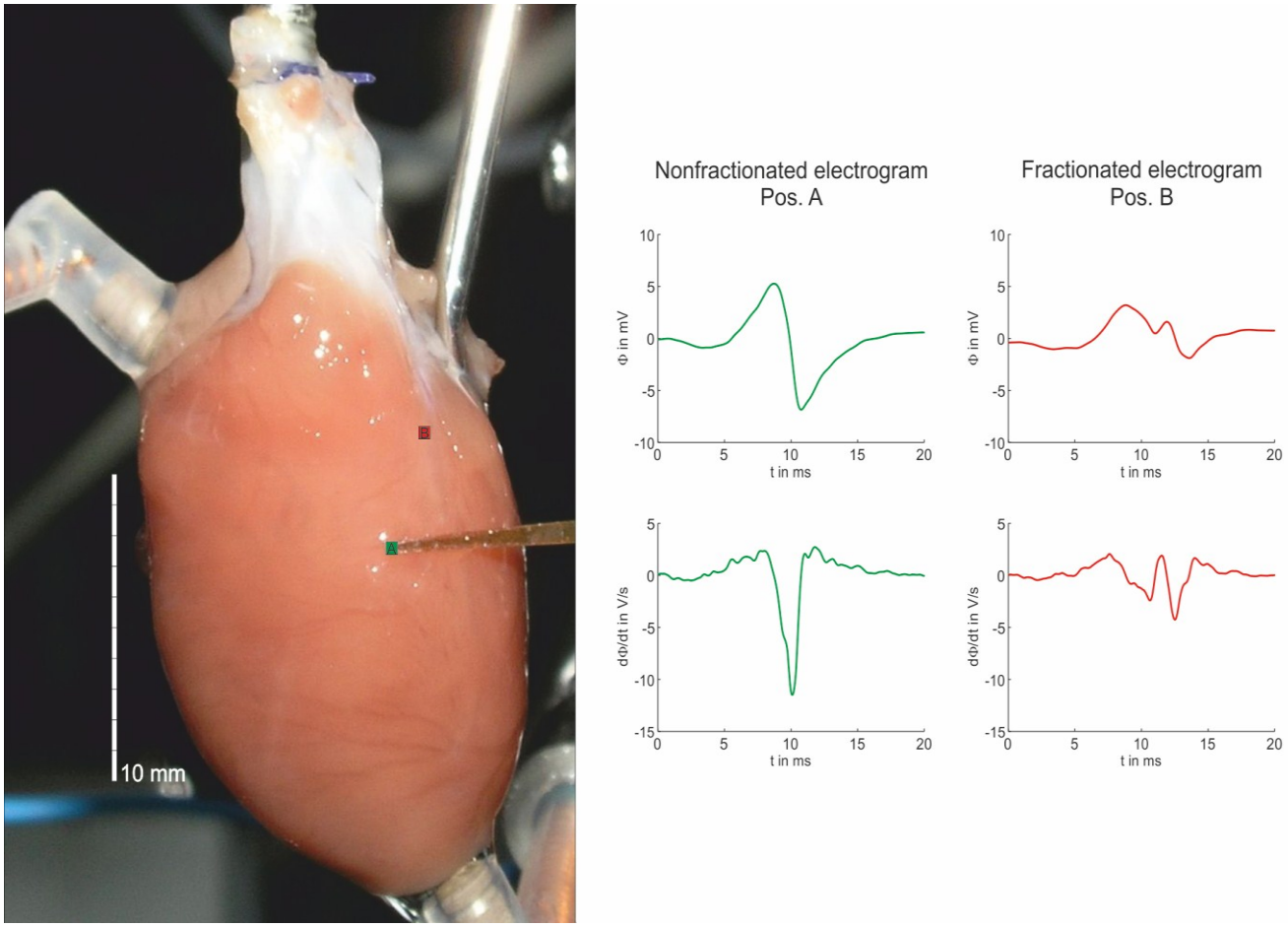

Exemplary representation of conduction changes (A representing normal myocardium, B representing ischemic myocardium)

$\Phi_e(t)$:

Sequential mapping of the epicardial left ventricle was performed by the sensor consecutively moving and recording for at least 2 heart beats. In total 155 $\Phi_e(t)$ were measured within the CsA group and 77within the control group. All of the included data were normally distributed. (p=0,012 in the CsA group and 0,017 in the control group). The Levene's test for equality of variances showed that the values were homogeneously distributed by p> 0, 05 (p=0,108). The requirements for t- test performance were given. T-test showed that there was a significant difference ($p < 0.05$) in $\Phi_e(t)$ between CsA and control group(p= 0,029). The box-blots graphically present the difference among CsA and control group.

Box Blot 1:

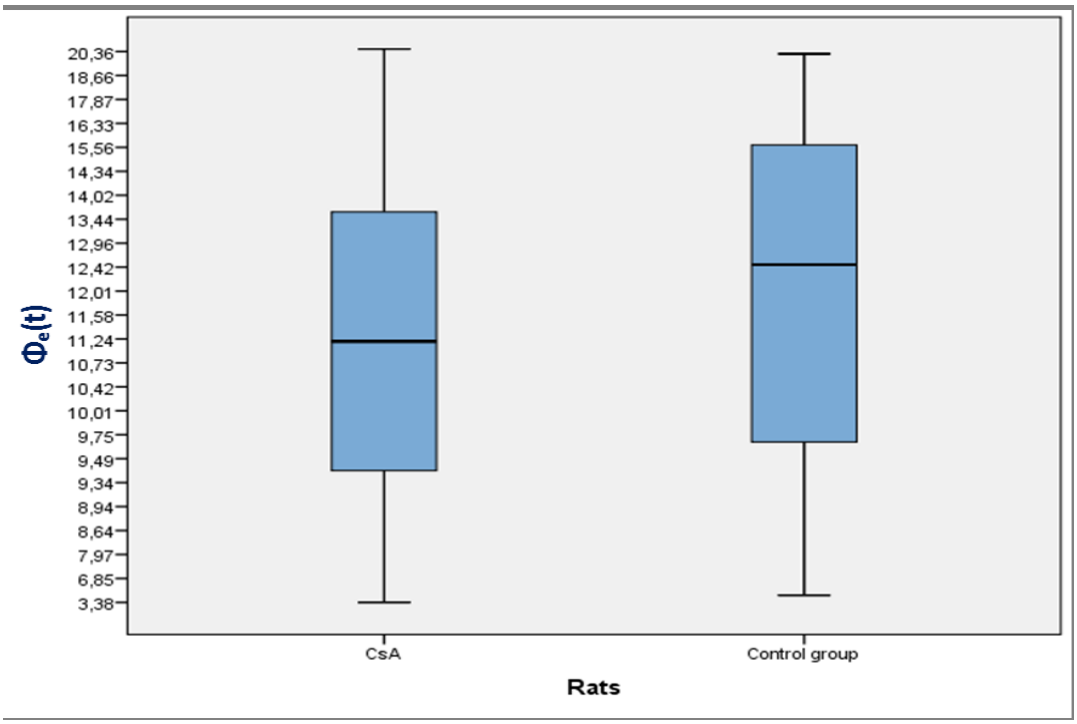

The CsA treated group showed a smaller mean value of $\Phi_e(t)$ as expected (mean $\Phi_e(t)$ = 11,6773 in the CsA is smaller than mean $\Phi_e(t)$ = 12,7576 in control group, p=0.005) .

$d\Phi_e(t)/dt$

For easier manipulation of $d\Phi_e(t)/dt$ due to negative value of this variable, we took the absolute value [n1…n_x] of the same. A total of 155 $d\Phi_e(t)/dt$ data were collected within the CsA group and 77 witin the control group. All of the included data were normally distributed (p=0,001) within the CsA group and (p= 0, 0001) within the control group. The Levene's test for equality of variances showed that the values are homogeneously distributed by p> 0, 05 (p=0,374). The requirements for t- test performance were given. T-test showed that there was a significant difference ($p < 0.05$) in $d\Phi_e(t)/dt$ between CsA and control group(p= 0,002). The difference between the CsA and the control group were demonstrated in box-blots for $d\Phi_e(t)/dt$ (hereby it is to understand that the $d\Phi_e(t)/dt$ is taken as absolute value of negative $d\Phi_e(t)/dt$) .

Box Blot 2:

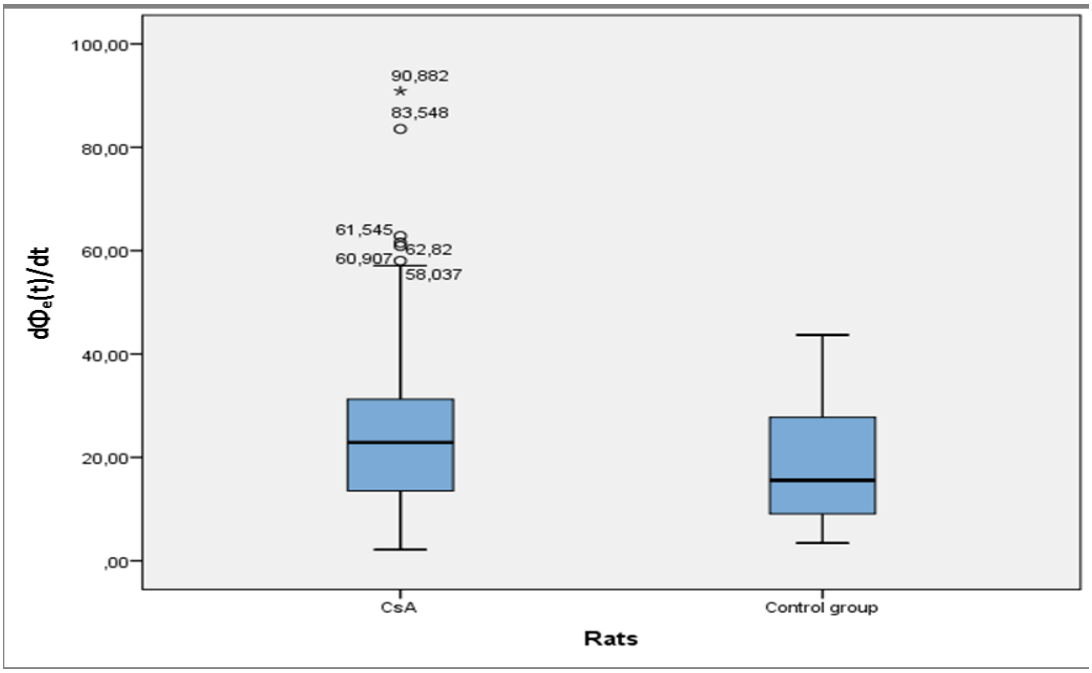

It was shown that the absolute value of $d\Phi_e(t)/dt$ is, as expected higher in the CsA group ($d\Phi_e(t)/dt$ = 24,5096) than in the control group($d\Phi_e(t)/dt$ = 18,6823, p=0,03), i.e. normal values of $d\Phi_e(t)/dt$ as negative are smaller in CsA group than in the control group.Extreme values of $d\Phi_e(t)/dt$ in box-blot which are shown just in the CsA treated group can all be related to two single rats.

Emag

A total of 155 Emag were measured in the CsA group and 77 in the control group. All of the included data were normally distributed (p=0,0001) CsA group and (p= 0, 001) control group. The Levene's test for equality of variances showed that the values are homogeneously distributed by p> 0, 05 (p=0,397). The requirements for t- test performance were given.

T-test showed that there was no significant difference (p < 0.05) in Emag between CsA and control group (p= 0,079).

This time we used the box-blots as graphical presentation, although the T- test was not significant, to show the extreme values that occured in the CsA group.

Box Blot 3:

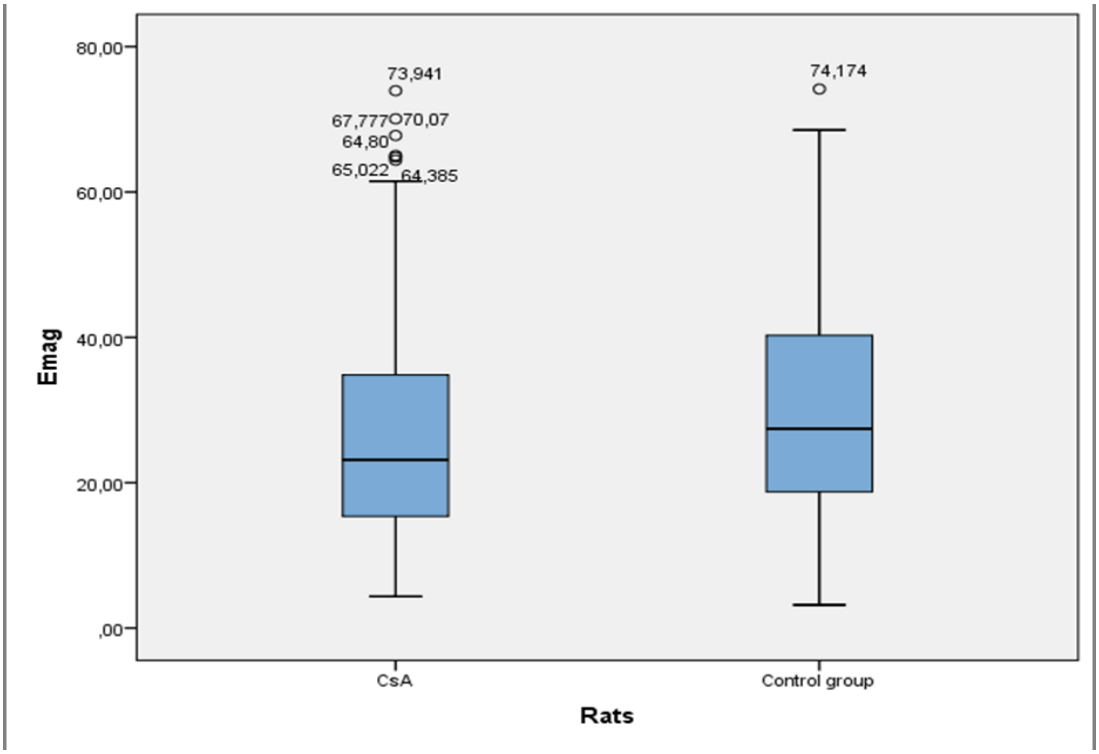

The extreme values could be subdivided to three single rats all of CsA group.

FI

For the variable of FI we calculated the percentage distribution for each discreet value (1-7) it could take, with the aim to show the distribution inside the group and to compare one group to each other. Considering that FI could be unfractionated (FI = 1), middle fractioned (FI= 2) or high fractioned (FI≥3). Total of 155 FI for the CsA group and 77 FI measurements for the control group were taken.

Table 5:

FI	Frequency in CsA group	Frequency in control group	Percentage CsA group	Percentage control group
no fractionation	120	41	77,4	53,2
middle-grade fractionation	31	28	20,0	36,4
high fractionation	4	8	2,6	10,4

As shown in the table both groups differ in percentage of represented possible values of FI.

It was shown that in both groups the percentage of unfractionated electrograms inside the groups was higher than middle fractionated ones (77,4% > 20,0 % for CsA group and 53,2 % > 36,4% for the control group, p=0.003), and the middle fractionated electrograms were higher present as the high fractionated electrograms (20,0% > 2,6% for the CsA group and 36,4 > 10,4 % for the control group (p=0.001)).

The comparison between the groups showed that high fractionated electrograms had a higher percentage in the control group than in the CsA treated group (10,4%>2,6%).
Same could be determined for the middle-grade fractionated electrograms (36,4% in the control group is higher than 20,0% within the CsA group (p=0.03)) .
Unfractionated electrograms were higher in the CsA treated group (77,4% >53,2%, p=0.03).

The graphical representation was used to show these differences inside each group

Graph 2:

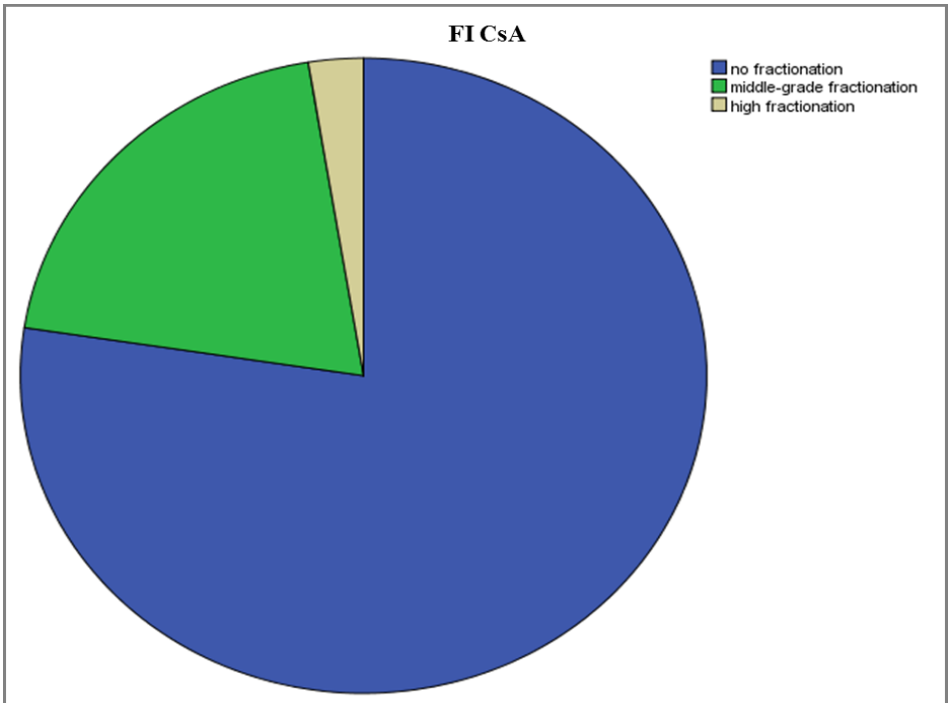

Graph 3:

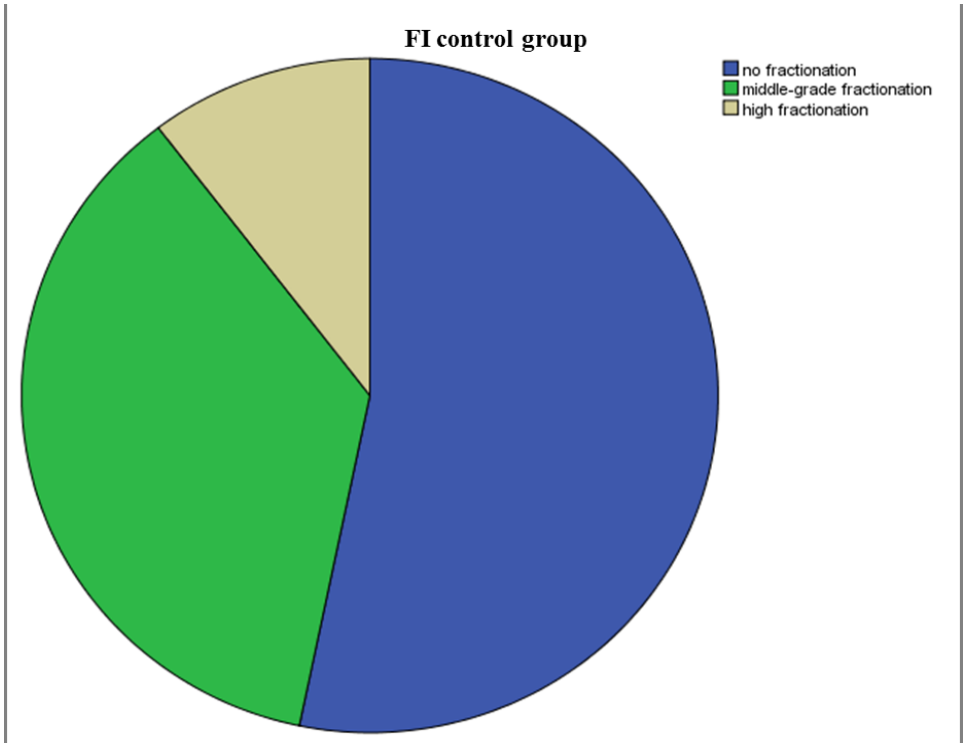
FI control group
no fractionation
middle-grade fractionation
high fractionation

4. 4 Histopathological Results

From the 3 CsA and 6 control rat hearts, the apex was harvested and divided into a total of 4 slices of 5 µm thickness for histopathological examination. HE and Masson's trichrome staining were applied for fibrosis diagnosis. In total 24 tissue preparations from the CsA and 12 tissue preparations from the control group were examined.

In 50 % of the CsA tissue samples minimal fibrosis was detected (1°: <5% minimal) whereas we could not detect any fibrosis in the tissue samples of the control hearts.

Below we show an exemplary representation of the histopathological findings :

Picture 1:

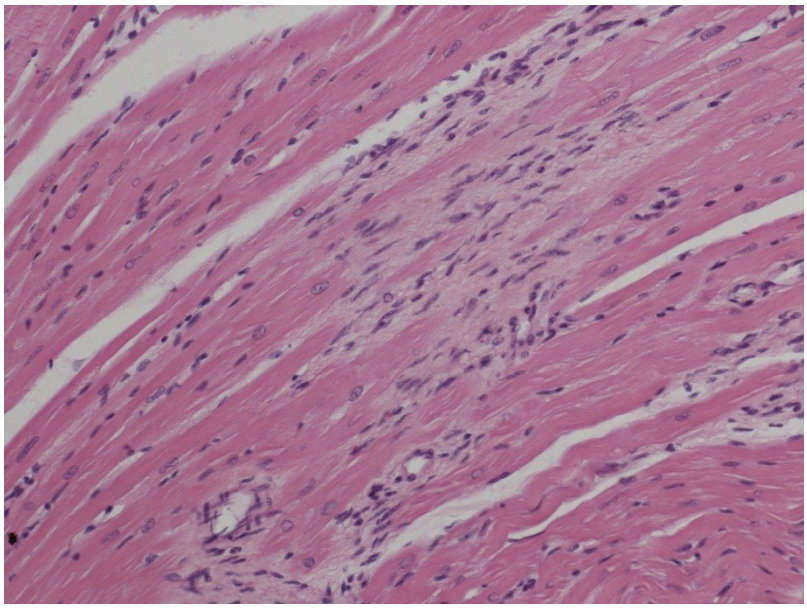

Rat heart of a CsA rat, left ventricle in haematoxylin–eosin stain with detected patchy fibrosis

Picture 2:

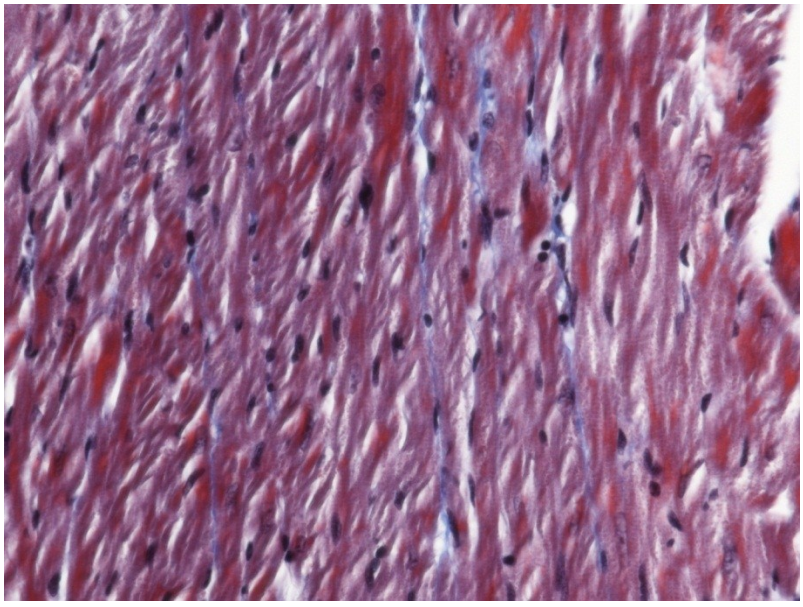

Same CsA treated rat, left ventricle in Masson's trichrome stain showing interstitial fibrosis

Pictures 3:

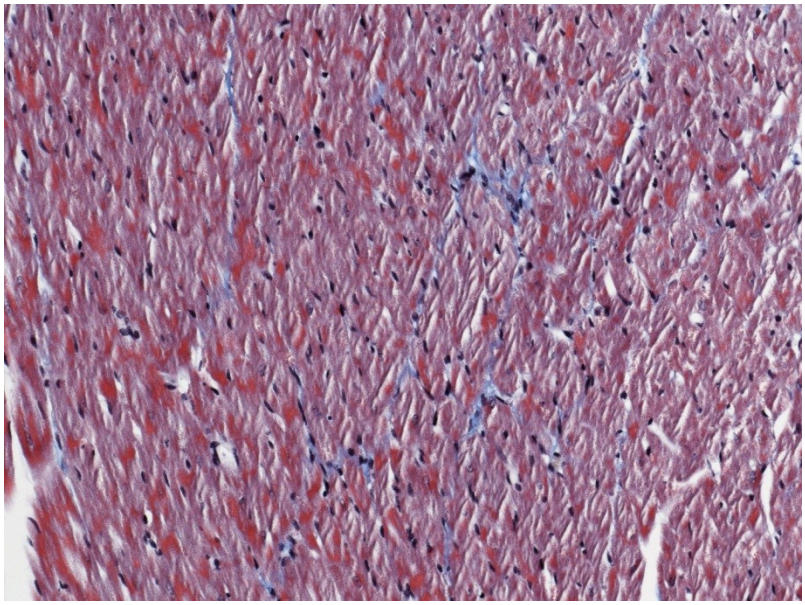

Exemplary rat heart slice from another CsA treated rat, left ventricle in Masson's trichrome stain showing interstitial fibrosis

Picture 4:

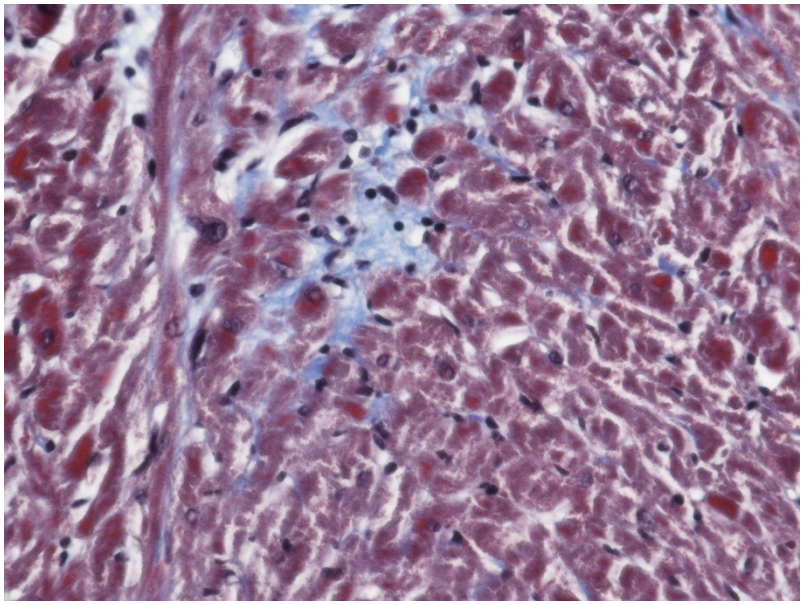

CsA treated rat, left ventricle in Masson's trichrome stain showing recent fibrosis

Picture 5:

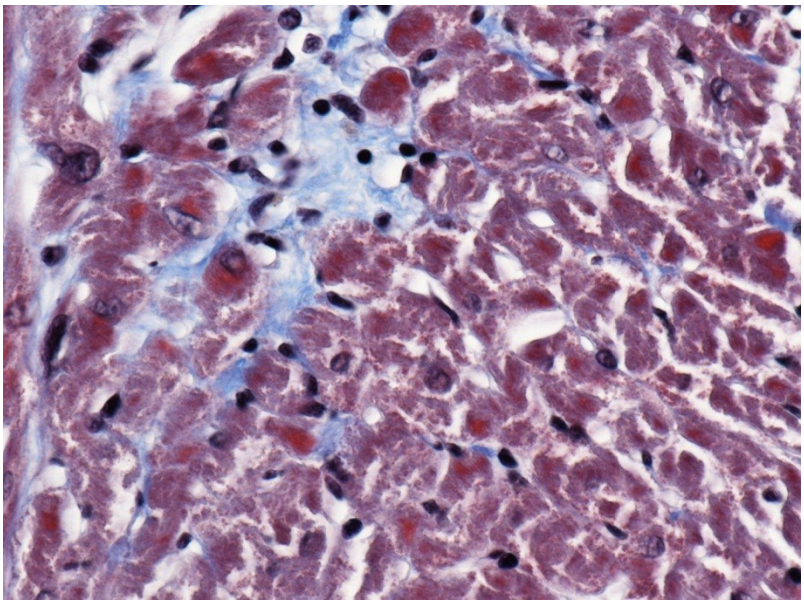

Same tissue sample as in picture 4, in higher magnification showing a better insight of recent fibrosis, recent fibrosis is presented by still present cell nuclei in high amount

5) DISCUSSION

Within the physiological data, no significance was found between the two formed groups.
The difference which was detected for the values of heart rate, i.e. main heart rate in the CsA treated group was higher than in the control group (257, 7967 bpm > 192, 5524 bpm, p=0.05), might just be considered as a normal variation of heart rate. As the values are still within the physiological range of heart rate for rats (250- 450 bpm) (77)
The impact of cyclosporine on the progression of cardiac fibrosis is controversially discussed throughout the literature. (17) (53) (61)
The histo-pathological findings showed areas of fibrosis in just 50% of the hearts. Furthermore the fibrotic areas were not extremely extended. Nevertheless these minor histological changes were detected by the sensor, thus achieving our two objectives. As expected these minor structural changes have not led to a pathological heart function yet. It can only be assumed that a larger amount of fibrosis would have led to pathological deterioration of the cardiac function caused either by an increase of the cyclosporine dosage or duration of the treatment.

Concerning the micro- conduction mapping measurements, the sensor was able to detect small amounts of fibrosis, thus showing a high sensitivity. Significant differences in almost all electrophysiological parameters could be determined. The mean value of $\Phi_e(t)$ for the CsA treated group was smaller, the absolute value of $d\Phi_e(t)/dt$ than in the control group.
Extreme values of $d\Phi_e(t)/dt$ were detected just in the CsA treated group and can all be subdivided to just two rats which respectively showed only a small gain of their body weight and subsequently of their heart weight.

Due to the large deviations from normal distribution no significance could be estimated for E mag. Nevertheless the main values of Emag were smaller within the CsA group compared to the control group. The extreme values could be attributed to just three rats of CsA group all being in the lower 50% range of the heart and body weight.
The index of FI showed that high fractionated electrograms had a higher percentage in the control group than in the CsA treated group.
The same could be determined for the middle-grade fractionated electrograms, while the unfractionated electrograms were higher in the CsA treated group.
Partly the correlation of extreme values for $d\Phi_e(t)/dt$ and Emag to the histo-pathological findings could be established.
Statistical analysis of electrical near field has shown that minor fibrosis, as the one that occurred in our study could be detected by this new method even though there were no changes evident in the physiological cardiac performance. The results for each variable tested are still difficult to paraphrase. The differences among CsA group and control group might be attributed to a few origins.

Some of the possible explantaions of these results could be the thickness of the liquid film on the surface of the medium where the measurements were performed, technical malfunctions, changes in membrane kinetics due to application of CsA and changes into microstructure of the heart i.e. fibrosis occurrence. At this point it still is not possible to tell which of these factors mentiones above are responsible for the detected changes.
It can be hypothesized that we succeeded to induce fibrosis and to detect the same with our measurement system thereby we could have one possible explanation for our results.

The proven decrease in surface potential $\Phi_e(t)$ in this case could be explained by the fact that by occurrence of fibrosis the amount of regular myocytes is smaller, i.e. the amount of cells contributing to a formation of surface potential is reduced which leads to the development of a decreased surface potential; whereas inside the myocardium, which consists of regular myocytes the surface potential is higher due to the outnumber of regular myocytes.
The value of $d\Phi_e(t)/dt$ also showed a decrease in the CsA treated group versus the control group; however due to extreme values which occur in the CsA treated group it still is not possible to make a valid statement about the underlying causes.
Results of Emag were too unequally distributed, and the extreme values in the CsA group made a valid statement impossible too.
Nevertheless, it can be estimated that we can attribute these extreme values to specific rats of the CsA group, which have shown the least increase in heart and bodyweight. This might implicate that the CsA treatment in those animals showed a higher effect by not letting them gain weight sufficiently. This could be partially confirmed by histological findings of fibrosis mostly in the same rat population.
For the value of FI it was expected that more fractionation would be detected in the CsA group than in the control group, due to fibrosis; while our results show the contrary situation.

In summary the results show that CsA levels and CsA administration definitely do have an implication on the acquaintance of fibrosis in cardiac tissue. Nevertheless due to the mostly inhomogeneous distribution of the measured sizes further investigations in order to get a better understanding and knowledge of the underlying process is definitely required.

6) CONCLUSION AND PERSPECTIVE

Considering the fact that microstructure related arrhythmias will increase with an increase in life expectancy, the minimal invasive tools to detect the amount and location of microstructural changes might gain importance. Procedures applied in human cardiac surgery can be used in animal experiments and thereby help to predict the potential diagnostic and therapeutic power of this new micro-conduction measurement method.

Generally our results fulfil our expectations by the fact that discreet fibrosis, as histologically determined, could be detected by the sensor. This confirms the sensitivity of this new sensor and indicates its value for catheter ablation. The new knowledge about micro- conduction gained by this method might become important in clinical application in the future.

Nevertheless further research is necessary to be able to make valid statements of the efficiency and reproducibility of this method. Considering the occurrence of extreme values of electrical near field measurements in the CsA treated group and just partially proven fibrosis inside of CsA group by histo-pathological finding one option would be to prolong the treatment with CsA thus achieving a more homogenous distribution of fibrosis throughout the tissue. Furthermore it would be necessary to enlarge the number of treated animals, which does not meet the ethical criteria. Therefore another protocol to induce massive cardiac fibrosis should be preferred in future studies using more effective agents, like isoproterenol. (78) (79)

Considering the improvement of the measurement systems a new computer model has already been established as described below.

6.1New Computer Model

A new hypothesis has been made with aim to improve the impact of this new micro conduction measurement method.

Local recordings of extracellular signals obtained with cardiac near-field sensors could reveal structural properties, such as microfibrosis by applying electrical stimuli around the sensor and analysing the directional dependence of signal parameters.

A recent computer simulation study has confirmed this hypothesis (80)

In this work the tissue was paced at twice threshold current and the signal amplitude and fractionation index were analysed. The evaluated parameters showed the expected directional dependence. In tissue with multidirectional oriented obstacles the signal amplitude had low values and the fractionation index was high, while in well coupled tissue this was not the case.

Latest experiments on isolated tissue preparations are promising in confirming the results of this computer study and therefore enable to correlate the directional dependency of extracellular potentials and the underlying microscopic tissue structure to characterize micro fibrosis.

7) LITERATURE

1. European cardiovascular disease statistics. *www.ehnheart.org/cvd-statistics.html.* [Online]

2. European society of cardiology. *www.eurekalert.org/pub_releases/2008-02/esoc-tha022008.php.* [Online]

3. WHO; http://www.who.int/healthinfo/global_burden_disease/estimates_country/en/index.html. *Death and DALY estimates for 2004 by cause for WHO Member States:Persons, all ages;death rates; Table 3. Estimated deaths per 100,000 population by cause, and Member State, 2004 (a).* [Online]

4. Statistisches Jahrbuch Österreichs; http://www.statistik.at/web_en/publications_services/statistisches_jahrbuch/index.html. *International data; Health; Share of total expenditure on health in GDP and per capita, US$ PPP in 2009.* [Online]

5. Statistisches Jahrbuch Österreichs; http://www.statistik.at/web_en/publications_services/statistisches_jahrbuch/index.html. *International data; Health; Age-standardized mortality rates by main causes in selected countries.* [Online]

6. Statistics Austria. *http://www.statistik.at/web_en/statistics/health/causes_of_death/causes_of_death_at_a_glance/index.html.* [Online]

7. WHO: International Statistical Classification of Diseases and Related Health Problems 10th Revision (ICD-10) Version for 2010. *http://apps.who.int/classifications/icd10/browse/2010/en#/IX.* [Online]

8. WHO; http://www.who.int/healthinfo/global_burden_disease/estimates_country/en/index.html. *Death and DALY estimates for 2004 by cause for WHO Member States:Persons, all ages;death rates;Table 5. Age-standardized death rates per 100,000 by cause, and Member State, 2004 (a, p).* [Online]

9. **Thygesen K, Alpert JS, White HD.** Universal definition of myocardial infarction. *European Heart Journal.* 2007 Oct, Vol. 28.

10. **Christine Jellis, MD, Jennifer Martin, MD, PhD, Jagat Narula, MD, PhD†, Thomas H. Marwick, MD, PhD.** Assessment of NonischemicMyocardialFibrosis. *Journal of the American College of Cardiology.* 56, 2010, Vol. 2.

11. **S. de Jong, T. A. B. van Veen, J. M. T. de Bakker and H. V. M. van Rijen.** Monitoring cardiac fibrosis: a technical challenge. *Neth Heart J.* 20(1), 2012 January.

12. **Tan, Alex Y MD and Zimetbaum, Peter MD.** Atrial Fibrillation and Atrial Fibrosis. *Journal of Cardiovascular Pharmacology.* 57, 2011, Vol. 6.

13. **Fauci, A.S., et al.** *Harrisons Innere Medizin, Band 1,2 ;17 Auflage .* Berlin : ABW Wissenschaftsverlag, 2008.

14. **de Jong S, van Veen TA, van Rijen HV, de Bakker JM.** Fibrosis and cardiac arrhythmias. *J Cardiovasc Pharmacologie.* 2011, Vol. 57(6).

15. **Everett TH 4th, Olgin JE.** Atrial fibrosis and the mechanisms of atrial fibrillation. *Heart Rhythm.* 4(3 Suppl), 2007.

16. **AG., Jardine.** Assessing the relative risk of cardiovascular disease among renal transplant patients receiving tacrolimus or cyclosporine. *Transpl Int.* 18(4), 2005.

17. **Stacchiotti A, Bonomini F, Lavazza A, Rodella LF, Rezzani R.** Adverse effects of cyclosporine A on HSP25, alpha B-crystallin and myofibrillar cytoskeleton in rat heart. *Toxicology.* 21;262(3), 2009.

18. **Yao Sun, Karl T. Weber.** Animal Models of Cardiac Fibrosis. *Methods in Molecular Medicine .* 117, 2005.

19. **de Jong, Sanne MSc, et al.** Biomarkers of Myocardial Fibrosis. *Journal of Cardiovascular Pharmacology.* 57, 2011.

20. University of Utah health sciences. *Utah classification.* [Online] [Cited: 28 Mai 2012.] http://healthsciences.utah.edu/carma/technology/Utah_Classification_AF.html.

21. **Khan R, Sheppard R.** Fibrosis in heart disease: understanding the role of transforming growth factor-beta in cardiomyopathy, valvular disease and arrhythmia. *Immunology.* 118, 2006, Vol. 1.

22. **Kuppahally SS, Akoum N, Burgon NS, Badger TJ, Kholmovski EG, Vijayakumar S, Rao SN, Blauer J, Fish EN, Dibella EV, Macleod RS, McGann C, Litwin SE, Marrouche NF.** Left atrial strain and strain rate in patients with paroxysmal and persistent atrial fibrillation: relationship to left atrial structural remodeling detected by delayed-enhancement MRI. *Circulation Cardiovascular Imaging.* 3, 2010, Vol. 3.

23. WHO:International Statistical Classification of Diseases and Related Health Problems 10th Revision (ICD-10) Version for 2010:Other forms of heart disease. *http://apps.who.int/classifications/icd10/browse/2010/en#/I30-I52.* [Online]

24. **Renate B Schnabel MD, Prof Lisa M Sullivan PhD , Prof Daniel Levy MD , Michael J Pencina PhD , Joseph M Massaro PhD , Prof Ralph B D'Agostino , Christopher Newton-Cheh MD , Jennifer F Yamamoto MA , Jared W Magnani MD , Thomas M T.** Development of a risk score for

atrial fibrillation (Framingham Heart Study): a community-based cohort study. *The Lancet.* 373, 2009.

25. **Kannel WB, Wolf PA, Benjamin EJ, Levy D.** Prevalence, incidence, prognosis, and predisposing conditions for atrial fibrillation: population-based estimates. *American Journal of Cardiolgy.* 82, 1998, Vol. 8A.

26. **Miyasaka Y, Barnes ME, Gersh BJ, Cha SS, Bailey KR, Abhayaratna WP, Seward JB, Tsang TS.** Secular trends in incidence of atrial fibrillation in Olmsted County, Minnesota, 1980 to 2000, and implications on the projections for future prevalence. *Circulation.* 114, 2006, Vol. 2.

27. **Macfarlane PW, Murray H, Sattar N, Stott DJ, Ford I, Buckley B, Jukema JW, Westendorp RG, Shepherd J.** The incidence and risk factors for new onset atrial fibrillation in the PROSPER study. *Europace.* 13, 2011, Vol. 5.

28. **Go AS, Hylek EM, Phillips KA, Chang Y, Henault LE, Selby JV, Singer DE.** Prevalence of diagnosed atrial fibrillation in adults: national implications for rhythm management and stroke prevention: the AnTicoagulation and Risk Factors in Atrial Fibrillation (ATRIA) Study. *JAMA.* 285, 2001, Vol. 18.

29. **Nattel S, Shiroshita-Takeshita A, Brundel BJ, Rivard L.** Mechanisms of atrial fibrillation: lessons from animal models. *Progress in Cardiovascular Diseases.* 48, 2005, Vol. 1.

30. **Eric J. Topol, Robert M. Califf, Eric N. Prystowsky and James D. Thomas.** *Textbook of Cardiovascular Medicine.* Philadelphia : Lippincott Williams & Wilkins , 2007.

31. **Thorsten Lewalter, Berndt Lüderitz.** *Herzrhythmusstörungen: Diagnostik und Therapie.* Berlin : Springer Verlag, 2010.

32. **Hindricks G, Kircher S, Gaspar T,Arya A.** Therapie von Vorhofflimmern: Rolle der Katheterablation. *Journal für Kardiologie - Austrian Journal of Cardiology.* 16,Supp A, 2009.

33. **Meyer C, Martinek M,Pürerfellner H.** Katheterablation ventrikulärer Tachykardien. *Journal für Kardiologie - Austrian Journal of Cardiology.* 18, 2011, Vols. 3-4.

34. **Arora R., Das M. K., Zipes D. P., Wu J.** Optical Mapping Of Cardiac Arrhythmias. *Indian Pacing Electrophisiol J.* 3, 2003, Vol. 4.

35. **Derek J. Dosdall.** Cardiac Arrhythmia Mapping Chalenges and Opportunities. [Online] University of Utah, 22 October 2010. http://www.sci.utah.edu/~macleod//bioen/be6460/notes/W07-mapping.pdf.

36. **Jacquemet V, Henriquez CS.** Genesis of complex fractionated atrial electrograms in zones of slow conduction: a computer model of microfibrosis. *Heart Rhythm.* 6, 2009, Vol. 6.

37. **Plank G, Hofer E.** Model study of vector-loop morphology during electrical mapping of microscopic conduction in cardiac tissue. *Annals of Biomedical Engineering.* 28, 2000, Vol. 10.

38. **Spach M S, Dolber P C.** Relating extracellular potentials and their derivatives to anisotropic propagation at a microscopic level in human cardiac muscle. Evidence for electrical uncoupling of side-to-side fiber connections with increasing age. *Circ res.* 58, 1986, Vol. 3.

39. **Hofer E, Wiener T, Prassl AJ, Thurner T, Plank G.** Oblique propagation of activation allows the detection of uncoupling microstructures from cardiac near field behavior. *Conf Proc IEEE Eng Med Biol Soc.* 2007.

40. **E. Hofer, F. Keplinger, T. Thurner, T. Wiener, D. Sanchez-Quintana, V. Climent and G. Plank.** A new floating sensor array to detect electric near fields of beating heart preparations. *Biosensors and Bioelectronics.* 21, 2006.

41. **R. Arnold, T. Wiener, T. Thurner, E. Hofer.** A Novel Electrophysiological Measurement System to Study Rapidly Paced Animal Hearts . [book auth.] Pascal Verdonck, Marc Nyssen, Jens Haueisen Jos van der Sloten. *4th European Conference of the International Federation for Medical and Biological Engineering 23 - 27 November 2008, Antwerp, Belgium.* s.l. : Springer, 2008.

42. **Wiener, T, Arnold, R and Hofer, E.** On-line analysis of cardiac near field signals during electrophysiological experiments with heart preparations. *International Instrumentation and Measurement Technology Conference.* 2012, ISBN: 4577-1771.

43. **Campos FO, Wiener T, Prassl AJ, Ahammer H, Plank G, Weber Dos Santos R, Sánchez-Quintana D, Hofer E.** A 2D-computer model of atrial tissue based on histographs describes the electro-anatomical impact of microstructure on endocardiac potentials and electric near-fields. *Conf Proc IEEE Eng Med Biol Soc.* 2010.

44. **Skrzypiec-Spring M, Grotthus B, Szelag A, Schulz R.** Isolated heart perfusion according to Langendorff---still viable in the new millennium. *J Pharmacol Toxicol Methods.* 55, 2007, Vol. 2.

45. **HJ, Döring.** The isolated perfused heart according to Langendorff technique--function--application. *Physiol Bohemoslov.* 39, 1990, Vol. 6.

46. **Liao R, Podesser BK, Lim CC.** The continuing evolution of the Langendorff and ejecting murine heart: new advances in cardiac phenotyping. *Am J Physiol Heart Circ Physiol.* 303, 2012, Vol. 2.

47. **Dehnert, H. J. Döring and H.** *Das isolierte perfundierte Warmblüter-Herz nach Langendorff.* March : Biomesstechnik-Verl., 1985. ISBN 3-924638-04-7.

48. **Langendorff, O.** *Untersuchungen am ueberlebenden Saeugethierherzen. Pfluegers Archiv , (61):291-332, 1895.* Bonn : Pfluegers Archiv , Band 61, 1895.

49. **Schlich, Thomas.** *Die Erfindung der Organtransplantation: Erfolg und Scheitern des chirurgischen Organersatzes(1880-1930).* Frankfurt/Mein;New York : Campus Verlag, 1998 . ISBN 3-593-35940-5.

50. **Robert Pfitzmann, Peter Neuhaus ,Roland Hetzer.** *Organtransplantation:Transplantation thorakaler und abdomineller Organe.* Berlin;New York : de Gruyter, 2001 . ISBN 3-11-016849-9.

51. **HF, Stähelin.** The history of cyclosporin A (Sandimmune) revisited: another point of view. *Experientia.* 52, 1996, Vol. 1.

52. **Wenger, Roland M.** Synthesis of cyclosporine. Total syntheses of 'cyclosporin A' and 'cyclosporin H', two fungal metabolites isolated from the species Tolypocladium inflatum GAMS. *Helvetica Chimica Acta.* 67, 1984, Vol. 2.

53. **Rezzani, Rita.** Cyclosporine A and adverse effects on organs: histochemical studies. *Progress in Histochemistry and Cytochemistry.* 9, 2004, Vol. 2.

54. Mechanism of Action of Cyclosporine or Tacrolimus (FK 506). Cambridge University Press *Expert Reviews in Molecular Medicine.* s.l. : Cambridge University Press, 2000.

55. **Stenvinkel P, Carrero JJ, Axelsson J, Lindholm B, Heimbürger O, Massy Z.** Emerging biomarkers for evaluating cardiovascular risk in the chronic kidney disease patient: how do new pieces fit into the uremic puzzle? *Clin J Am Soc Nephrol.* 3, 2008, Vol. 2.

56. **Rezzani R, Rodella LF, Fraschini F, Gasco MR, Demartini G, Musicanti C, Reiter RJ.** Melatonin delivery in solid lipid nanoparticles: prevention of cyclosporine A induced cardiac damage. *J Pineal Res.* 46, 2009, Vol. 3.

57. **Jurado F, Bellón JM, Pareja JA, Golitsin A, Millán L, Pascual G, Buján J.** Effects of ischaemia-reperfusion and cyclosporin-A on cardiac muscle ultrastructure. *Histology and yhistopathology.* 13, 1998, Vol. 3.

58. **Kostin S, Hein S, Arnon E, Scholz D, Schaper J.** The cytoskeleton and related proteins in the human failing heart. *Heart Failure Reviews.* 5, 2000, Vol. 3.

59. **Rezzani R, Rodella L, Dessy C, Daneau G, Bianchi R, Feron O.** Changes in Hsp90 expression determine the effects of cyclosporine A on the NO pathway in rat myocardium. *FEBS Letters.* 552, 2003, Vols. 2-3.

60. **Seung Ho Lee, Sang June Hahn,Gyesik Min, Jimok Kim,Su-Hyun Jo, Han Choe,and Bok Hee Choi.** Inhibitory Actions of HERG Currents by the Immunosuppressant Drug Cyclosporin A. *Korean Journal of Physiological Pharmacologie.* 15, 2011, Vol. 5.

61. **Xie JR, Yu LN.** Cardioprotective effects of cyclosporine A in an in vivo model of myocardial ischemia and reperfusion. *Acta Anaesthesiologica Scandinavica.* 51, 2007, Vol. 7.

62. **Young BA, Burdmann EA, Johnson RJ, Andoh T, Bennett WM, Couser WG, Alpers CE.** Cyclosporine A induced arteriolopathy in a rat model of chronic cyclosporine nephropathy. *Kidney Int.* 48, 1995, Vol. 2.

63. **Montaigne D, Marechal X, Baccouch R, Modine T, Preau S, Zannis K, Marchetti P, Lancel S, Neviere R.** Stabilization of mitochondrial membrane potential prevents doxorubicin-induced cardiotoxicity in isolated rat heart. *Toxicol Appl Pharmacol.* 244, 2010, Vol. 3.

64. **Naderi R, Imani A, Faghihi M.** Phenylephrine produces late pharmacological preconditioning in the isolated rat heart. *Eur J Pharmacol.* 627, 2010, Vols. 1-3.

65. **HUME, C. W.** *The Legal Protection of Laboratory Animals. in: The UFAW Handbook on the Care and Management of Laboratory Animals.* UFAW, London : Worden and Lane-Pette, 1957.

66. West Virgina University,Office of research, integrity & compilance. *Animal Research and the ACUC ; IACUC Policies;Rat Anesthesia and Analgesia Guidelines .* [Online] http://oric.research.wvu.edu/r/download/114254.

67. **Gross, D.R.** *Animal Models in Cardiovascular Research, 3rd Edition.* New York : Springer Science + Business Media, LLC, 2009.

68. RESEARCH ANIMAL RESOURCES. *Anesthesia.* [Online] http://www.ahc.umn.edu/rar/anesthesia.html#Benzodiazapines.

69. *Guidelines to promote the wellbeing of animals used for scientific purposes;The assessment and alleviation of pain and distress in research animals.* [Online] 2008. http://www.nhmrc.gov.au/_files_nhmrc/publications/attachments/ea18.pdf?q=publications/synopses/_files/ea18.pdf.

70. **Christine Jellis, MD, Jennifer Martin, MD, PhD, Jagat Narula, MD, PhD†, Thomas H. Marwick, MD, PhD.** Assessment of NonischemicMyocardialFibrosis. *Journal of the American College of Cardiology.* 56, 2010 Jul, Vol. 2.

71. **Siegenthaler, W. and Blum, H.E.** *Klinische Pathophysiologie.* Stuttgart : Thieme Verlag, 2006.

72. **Thorsten Lewalter, Berndt Lüderitz.** *Herzrhythmusstörungen: Diagnostik und Therapie.* Heidelberg : Springer, 2010.

73. IHCWORLD. *Masson's Trichrome Staining Protocol for Collagen Fibers.* [Online] http://www.ihcworld.com/_protocols/special_stains/masson_trichrome.htm.

74. IHC WORLD. *Hematoxylin and Eosin (H&E) Staining Protocol.* [Online] http://www.ihcworld.com/_protocols/special_stains/h&e_ellis.htm.

75. **Bucher, O. and Wartenberg, H.** *Cytologie, Histologie und mikroskopische Anatomie des Menschen;12., vollst. überarb. Aufl.* Bern;Gottingen;Toronto;Seattle : Hans Huber Verlag, 1997. ISBN 3-456-82785-7.

76. DailyMed. *Sandimmune.* [Online] http://dailymed.nlm.nih.gov/dailymed/lookup.cfm?setid=5e5926a7-1de0-4b54-a5c0-286b6200ff82.

77. **E.D., Olfert, M., Cross B. and A.A., McWilliam.** Guide to the Care and Use of Experimental Animals. *Canadian Council on Animal Care.* 1993, Vols. Vol. 1, 2nd.

78. **Benjamin IJ, Jalil JE, Tan LB, Cho K, Weber KT, Clark WA.** Isoproterenol-induced myocardial fibrosis in relation to myocyte necrosis. *Circ Res.* 65, 1989, Vol. 3.

79. **Ferreira AJ, Castro CH, Guatimosim S, Almeida PW, Gomes ER, Dias-Peixoto MF, Alves MN, Fagundes-Moura CR, Rentzsch B, Gava E, Almeida AP, Guimarães AM, Kitten GT, Reudelhuber T, Bader M, Santos RA.** Attenuation of isoproterenol-induced cardiac fibrosis in transgenic rats harboring an angiotensin-(1-7)-producing fusion protein in the heart. *Ther Adv Cardiovasc Dis.* 4, 2010, Vol. 2.

80. **al, Campos F.O. et.** A 2D-computer model of atrial tissue based on histographs describe the electro-anatomical impact of microstructure on endocardiac potentials and electric near-fields. *Conf Proc IEEE Eng Med Bio Soc .* 2010.